Fondazione IRCCS Policlinico San Matteo — Sistema Socio Sanitario Regione Lombardia

REGOLE VALUTAZIONE TITOLI

ALLEGATO 2

CONCORSO PUBBLICO PER TITOLI ED ESAMI PER L'ASSUNZIONE A TEMPO INDETERMINATO E PIENO DI N.1 UNITÀ NEL PROFILO DI "DIRIGENTE MEDICO – DISCIPLINA DI NEURORADIOLOGIA" DA ASSEGNARE SC RADIOLOGIA DIAGNOSTICA PER IMMAGINI 2 - NEURORADIOLOGIA(2025-1.4.2/78)

CARRIERA (max 10,000 punti)

arrotonda periodi superiori ai 15 gg a 1 mesi

Cod.	Regola	Punti	x mesi	Tipo calcolo	Unità mis.	Omog.	Sovr.	% val.
100	Specializzazione conseguita ai sensi del D.Lgs 368/99	1,000	12	PRC	mesi	Si	No	100
101	Specializzazione conseguita ai sensi del D.Lgs 257/91	0,500	12	PRC	mesi	Si	Si	100
102	Borsa di Studio per la ricerca nella disciplina presso IRCCS pubblici /Università	0,250	12	PRC	mesi	Si	Si	100
103	Borsa di Studio per la ricerca in altra disciplina presso IRCCS pubblici /Università	0,125	12	PRC	mesi	Si	Si	100
104	Contratto a termine/Assegno per la ricerca nella disciplina	0,400	12	PRC	mesi	Si	Si	100
105	Contratto a termine/Assegno per la ricerca in altra disciplina	0,200	12	PRC	mesi	Si	Si	100
110	Presso SSN nella disciplina t.pieno	1,000	12	PRC	mesi	Si	Si	100
111	Presso SSN in disciplina affine t.pieno	0,750	12	PRC	mesi	Si	Si	100
112	Presso SSN in altra disciplina t.pieno	0,500	12	PRC	mesi	Si	Si	100
113	Presso IRCCS nella disciplina t.pieno	1,200	12	PRC	mesi	Si	Si	100
114	Presso IRCCS in disciplina affine t.pieno	0,900	12	PRC	mesi	Si	Si	100
115	Presso IRCCS in altra disciplina t.pieno	0,600	12	PRC	mesi	Si	Si	100
120	Presso SSN nella disciplina t.definito	0,800	12	PRC	mesi	Si	Si	100
121	Presso SSN in disciplina affine t.definito	0,600	12	PRC	mesi	Si	Si	100
122	Presso SSN in altra disciplina t.definito	0,400	12	PRC	mesi	Si	Si	100
123	Presso SSN in qualità di Specializzando nella disciplina	1,000	12	PRC	mesi	Si	Si	100
124	Presso SSN in qualità di Specializzando in disciplina affine	0,750	12	PRC	mesi	Si	Si	100
125	Presso SSN in qualità di Specializzando in altra disciplina	0,500	12	PRC	mesi	Si	Si	100
126	Presso IRCCS in qualità di Specializzando nella disciplina	1,200	12	PRC	mesi	Si	Si	100
127	Presso IRCCS in qualità di Specializzando in disciplina affine	0,900	12	PRC	mesi	Si	Si	100
128	Presso IRCCS in qualità di Specializzando in altra disciplina	0,600	12	PRC	mesi	Si	Si	100
130	Attività ambulatoriale interna nella disciplina	1,000	12	AMB	mesi	No	No	100
131	Attività ambulatoriale interna in disciplina affine	0,750	12	AMB	mesi	No	No	100
132	Attività ambulatoriale interna in altra disciplina	0,500	12	AMB	mesi	No	No	100
150	Presso PA come medico	0,500	12	PRC	mesi	Si	Si	100
160	Servizio militare/civile come medico	0,500	12	PRC	mesi	Si	Si	100
170	Presso Ente convenzionato/accreditato SSN nella disciplina	1,000	12	PRC	mesi	Si	Si	25
171	Presso Ente convenzionato/accreditato SSN in disciplina affine	0,750	12	PRC	mesi	Si	Si	25
172	Presso Ente convenzionato/accreditato SSN in altra disciplina	0,500	12	PRC	mesi	Si	Si	25
199	Titolo non valutabile	0,000	0	N	n.	No	No	100

ACCADEMICI E DI STUDIO (max 2,000 punti)

arrotonda periodi superiori ai 0 gg a 0 mesi

Cod.	Regola	Punti	x mesi	Tipo calcolo	Unità mis.	Omog.	Sovr.	% val.

REGOLE VALUTAZIONE TITOLI

CONCORSO PUBBLICO PER TITOLI ED ESAMI PER L'ASSUNZIONE A TEMPO INDETERMINATO E PIENO DI N.1 UNITÀ NEL PROFILO DI "DIRIGENTE MEDICO – DISCIPLINA DI NEURORADIOLOGIA" DA ASSEGNARE SC RADIOLOGIA DIAGNOSTICA PER IMMAGINI 2 - NEURORADIOLOGIA(2025-1.4.2/78)

200	Altra specializzazione in disciplina equipollente	2,000	0	EVE	n.	No	No	100
201	Altra specializzazione in disciplina affine	1,000	0	EVE	n.	No	No	100
202	Altra specializzazione in altra disciplina	0,500	0	EVE	n.	No	No	100
203	Ulteriore specializzazione in disciplina equipollente	0,500	0	EVE	n.	No	No	100
204	Ulteriore specializzazione in disciplina affine	0,250	0	EVE	n.	No	No	100
205	Ulteriore specializzazione in altra disciplina	0,125	0	EVE	n.	No	No	100
206	Dottorato di ricerca attinente	1,500	0	EVE	n.	No	No	100
207	Master universitario di II livello attinente	0,500	0	EVE	n.	No	No	100
219	Laurea come requisito di ammissione - non valutabile	0,000	0	N	n.	No	No	100
220	Altra laurea del ruolo sanitario fino ad un massimo di n. 2	0,750	0	EVE	n.	No	No	100
299	Titolo non valutabile	0,000	0	N	n.	No	No	100

PUBBLICAZIONI E TITOLI SCIENTIFICI (max 15,000 punti)

arrotonda periodi superiori ai 0 gg a 0 mesi

Cod.	Regola	Punti	x mesi	Tipo calcolo	Unità mis.	Omog.	Sovr.	% val.
300	Lavori in extenso con IF	0,300	0	EVE	n.	No	No	100
301	Lavori in extenso senza IF	0,050	0	EVE	n.	No	No	100
302	Abstract, poster comunicazioni a congressi	0,050	0	EVE	n.	No	No	100
303	Capitolo di libro internazionale	0,150	0	EVE	n.	No	No	100
304	Capitolo di libro nazionale	0,075	0	EVE	n.	No	No	100
305	Case Report - Lettere all'editore	0,100	0	EVE	n.	No	No	100
399	Lavori non valutabili	0,000	0	N	n.	No	No	100

CURRICULUM FORMATIVO E PROFESSIONALE (max 5,000 punti)

arrotonda periodi superiori ai 15 gg a 1 mesi

Cod.	Regola	Punti	x mesi	Tipo calcolo	Unità mis.	Omog.	Sovr.	% val.
400	Relatore/Responsabile scientifico/docente a corsi/congressi; tutor occasionale.	0,050	0	N	n.	No	No	100
401	Partecipazione a corsi, congressi di durata inferiore o pari a 50 ore	0,010	0	N	n.	No	No	100
402	Attività lavorativa subordinata e non subordinata presso Enti PRIVATI e/o PUBBLICI non ricompresa nei titoli di carriera, nella disciplina	0,400	12	PRC	mesi	Si	No	100
403	Attività lavorativa subordinata e non subordinata presso Enti PRIVATI e/o PUBBLICI non ricompresa nei titoli di carriera in disciplina affine	0,300	12	N	mesi	Si	No	100
404	Attività lavorativa subordinata e non subordinata presso Enti PRIVATI e/o PUBBLICI non ricompresa nei titoli di carriera quale medico	0,200	12	PRC	mesi	Si	No	100
405	Attività di guardia medica - medico assistenziale con indicazione ore	0,400	12	PRC	mesi	No	No	100
406	Borsa di studio presso Enti privati e Pubblici diversi da IRCSS pubblici o Università	0,200	12	PRC	mesi	No	No	100
407	Attività didattica accademica nella disciplina - dettaglio	0,000	0	N	n	No	No	100
408	Punteggio attività didattica accademica nella disciplina (0.500 punti forfait)	0,500	0	EVE	forfait	No	No	100

REGOLE VALUTAZIONE TITOLI

CONCORSO PUBBLICO PER TITOLI ED ESAMI PER L'ASSUNZIONE A TEMPO INDETERMINATO E PIENO DI N.1 UNITÀ NEL PROFILO DI "DIRIGENTE MEDICO – DISCIPLINA DI NEURORADIOLOGIA" DA ASSEGNARE SC RADIOLOGIA DIAGNOSTICA PER IMMAGINI 2 - NEURORADIOLOGIA(2025-1.4.2/78)

409	Attività di tutoraggio continuativo - dettaglio	0,000	0	N	n.	No	No	100
410	Punteggio attività di tutoraggio continuativo (0.400 punti forfait)	0,400	0	EVE	forfait	No	No	100
411	Partecipazione a progetti di ricerca/clinical trial/gruppi distudio	0,030	0	EVE	n.	No	No	100
412	Stage formativo all'estero in centri qualificati	0,300	0	EVE	n.	No	No	100
413	Attività professionalizzante all'estero nella disciplina	0,950	12	PRC	mesi	Si	Si	100
414	Premio di studio/Premio scientifico	0,100	0	EVE	n.	No	No	100
415	Diploma IUSS in ambito sanitario	0,500	0	EVE	n.	No	No	100
416	Dottorato di ricerca non attinente	0,500	0	EVE	n.	No	No	100
417	Cultore della materia	0,300	0	EVE	n.	No	No	100
418	Master universitario in ambito sanitario	0,500	0	EVE	n.	No	No	100
419	Corsi di perfezionamento - Corsi di durata superiore a 50 ore	0,400	0	N	n.	No	No	100
420	Frequenza volontaria, stage, tirocinio	0,000	0	EVE	n.	No	No	100
421	Partecipazione a corsi, congressi di durata superiore a 50 ore	0,040	0	N	n.	No	No	100
499	Titoli non valutabili	0,000	0	N	n.	No	No	100
501	Comprovata e specifica esperienza prevista dal bando - punteggio complessivo	2,000	0	N	n.	No	No	100
502	Comprovata e specifica esperienza prevista dal bando - dettaglio	0,000	0	N	n.	No	No	100

Sistema Socio Sanitario
Fondazione IRCCS Policlinico San Matteo
Regione Lombardia

PROVA NON ESTRATTA

[redacted]

2025-1.4.2/78

CONCORSO PUBBLICO PER TITOLI ED ESAMI PER L'ASSUNZIONE A TEMPO INDETERMINATO E PIENO DI N.1 UNITÀ NEL PROFILO DI "DIRIGENTE MEDICO – DISCIPLINA DI NEURORADIOLOGIA" DA ASSEGNARE SC RADIOLOGIA DIAGNOSTICA PER IMMAGINI 2 – NEURORADIOLOGIA

PROVA SCRITTA 1

Ictus ischemico acuto: considerazioni neuroradiologiche diagnostiche e terapeutiche

MAV cerebrali: definizione, diagnostica e principi di trattamento

C.C.S. FONDAZIONE I.R.C.S. POLICLINICO SAN MATTEO PAVIA

PROVA ESTRATTA

[redacted]

Sistema Socio Sanitario
Fondazione IRCCS Policlinico San Matteo
Regione Lombardia

2025-1.4.2/78

CONCORSO PUBBLICO PER TITOLI ED ESAMI PER L'ASSUNZIONE A TEMPO INDETERMINATO E PIENO DI N.1 UNITÀ NEL PROFILO DI "DIRIGENTE MEDICO – DISCIPLINA DI NEURORADIOLOGIA" DA ASSEGNARE SC RADIOLOGIA DIAGNOSTICA PER IMMAGINI 2 – NEURORADIOLOGIA

PROVA SCRITTA 2

Tumori pediatrici della fossa cranica posteriore: quadri neuroradiologici e diagnostica differenziale

Il vasospasmo post-ESA

I.R.C.S. - FONDAZIONE POLICLINICO SAN MATTEO PAVIA

PROVA NON SVOLTA

[redacted]

Sistema Socio Sanitario
Fondazione IRCCS Policlinico San Matteo
Regione Lombardia

2025-1.4.2/78

CONCORSO PUBBLICO PER TITOLI ED ESAMI PER L'ASSUNZIONE A TEMPO INDETERMINATO E PIENO DI N.1 UNITÀ NEL PROFILO DI "DIRIGENTE MEDICO – DISCIPLINA DI NEURORADIOLOGIA" DA ASSEGNARE SC RADIOLOGIA DIAGNOSTICA PER IMMAGINI 2 – NEURORADIOLOGIA

PROVA SCRITTA 3

Quadri neuroradiologici nel follow-up dei tumori cerebrali trattati

Fistole liquorali spinali: quali sono le tecniche diagnostiche di scelta e le opzioni di trattamento

F.C.S. - FONDAZIONE POLICLINICO SAN MATTEO PAVIA

2025-1.4.2/78

CONCORSO PUBBLICO PER TITOLI ED ESAMI PER L'ASSUNZIONE A TEMPO INDETERMINATO E PIENO DI N.1 UNITÀ NEL PROFILO DI "DIRIGENTE MEDICO – DISCIPLINA DI NEURORADIOLOGIA" DA ASSEGNARE SC RADIOLOGIA DIAGNOSTICA PER IMMAGINI 2 – NEURORADIOLOGIA

PROVA PRATICA 1

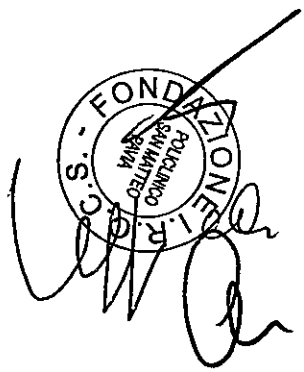

NON ESTRATTA [redacted]

Sistema Socio Sanitario
Fondazione IRCCS Policlinico San Matteo
Regione Lombardia

2025-1.4.2/78

CONCORSO PUBBLICO PER TITOLI ED ESAMI PER L'ASSUNZIONE A TEMPO INDETERMINATO E PIENO DI N.1 UNITÀ NEL PROFILO DI "DIRIGENTE MEDICO – DISCIPLINA DI NEURORADIOLOGIA" DA ASSEGNARE SC RADIOLOGIA DIAGNOSTICA PER IMMAGINI 2 – NEURORADIOLOGIA

PROVA PRATICA 2

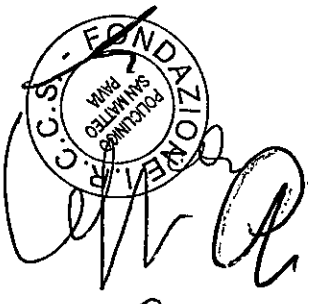

PROVA ESTRATTA [redacted]

Sistema Socio Sanitario
Fondazione IRCCS Policlinico San Matteo
Regione Lombardia

2025-1.4.2/78

CONCORSO PUBBLICO PER TITOLI ED ESAMI PER L'ASSUNZIONE A TEMPO INDETERMINATO E PIENO DI N.1 UNITÀ NEL PROFILO DI "DIRIGENTE MEDICO – DISCIPLINA DI NEURORADIOLOGIA" DA ASSEGNARE SC RADIOLOGIA DIAGNOSTICA PER IMMAGINI 2 – NEURORADIOLOGIA

PROVA PRATICA 3

FONDAZIONE I.R.C.C.S. POLICLINICO SAN MATTEO PAVIA

[redacted]

PROVA NON ESTRATTA

ALLEGATO 11

Sistema Socio Sanitario
Fondazione IRCCS Policlinico San Matteo
Regione Lombardia

2025-1.4.2/78

CONCORSO PUBBLICO PER TITOLI ED ESAMI PER L'ASSUNZIONE A TEMPO INDETERMINATO E PIENO DI N.1 UNITÀ NEL PROFILO DI "DIRIGENTE MEDICO – DISCIPLINA DI NEURORADIOLOGIA" DA ASSEGNARE SC RADIOLOGIA DIAGNOSTICA PER IMMAGINI 2 – NEURORADIOLOGIA

PROVA ORALE

1. Angiopatia amiloidea cerebrale
2. Fistole durali spinali
3. Angiomi cavernosi
4. Tumori della Regione sellare
5. Tumori cerebrali epilettogeni
6. Ematomi sottodurali
7. Ematoma epidurale classico
8. Ematomi intraparenchimali
9. Inquadramento neuroradiologico dell'ESA non traumatica
10. Classificazione delle fratture cervicali e iter diagnostico
11. Aneurismi intracranici
12. Sclerosi Multipla: criteri diagnostici e aspetti neuroradiologici
13. Dissecazioni carotidee
14. NF1: principali caratteristiche neuroradiologiche
15. Posterior reversible encephalopathy syndrome (PRES): considerazioni neuroradiologiche

FONDAZIONE I.R.C.C.S. POLICLINICO SAN MATTEO PAVIA

2025-1.4.2/78

CONCORSO PUBBLICO PER TITOLI ED ESAMI PER L'ASSUNZIONE A TEMPO INDETERMINATO E PIENO DI N.1 UNITÀ NEL PROFILO DI "DIRIGENTE MEDICO – DISCIPLINA DI NEURORADIOLOGIA" DA ASSEGNARE SC RADIOLOGIA DIAGNOSTICA PER IMMAGINI 2 – NEURORADIOLOGIA

16. Imaging neuroradiologico nel dolore lombare

17. Imaging neuroradiologico nel trauma cranico

18. Imaging neuroradiologico nel trauma spinale mielico

19. Patologia degenerativa della colonna vertebrale

20. Angio-TC e TC perfusione nello stroke ischemico

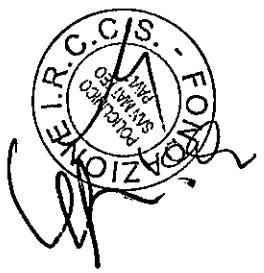

Sistema Socio Sanitario
Fondazione IRCCS Policlinico San Matteo
Regione Lombardia

ALLEGATO 12

2025-1.4.2/78

CONCORSO PUBBLICO PER TITOLI ED ESAMI PER L'ASSUNZIONE A TEMPO INDETERMINATO E PIENO DI N.1 UNITÀ NEL PROFILO DI "DIRIGENTE MEDICO – DISCIPLINA DI NEURORADIOLOGIA" DA ASSEGNARE SC RADIOLOGIA DIAGNOSTICA PER IMMAGINI 2 – NEURORADIOLOGIA

PROVA DI INFORMATICA

1. - **A QUANTO CORRISPONDE UN KILOBYTE?** Circa 1000 byte
2. - **CHE COSA E' LA FIRMA DIGITALE?** Un metodo di autenticazione personale di documenti elettronici
3. - **CHE COSA E' LO "SCANDISK"?** Un processo di controllo del disco fisso
4. - **COSA SONO LE "FAQ"?** Sono raccolte di risposte a domande che vengono poste spesso affrontando un argomento
5. - **CHE COS'E' L'HTML?** Il linguaggio che caratterizza le pagine web
6. - **CHE TIPO DI COMPUTER E' IL NOTEBOOK?** Portatile
7. - **CHE TIPO DI FILE HA COME ESTENSIONE "*.JPG":** Un file immagine
8. - **CHE TIPO DI FILE HA COME ESTENSIONE ".EXE":** Un file eseguibile
9. - **COME E' POSSIBILE SPOSTARE UN FILE CONTENUTO IN UNA CARTELLA DEL DISCO FISSO IN UN' ALTRA CARTELLA?** Trascinando l'icona del file sull'icona della cartella di destinazione
10. - **COMPRIMERE UN FILE SIGNIFICA:** Ridurre la dimensione del file
11. - **COSA E' L'"E-MAIL"?** Un servizio internet grazie al quale è possibile inviare o ricevere messaggi
12. - **COSA E' L'"IP ADDRESS"?** Un indirizzo IP identifica univocamente uno specifico computer
13. - **COSA E' LO "SPAM"?** Un messaggio non richiesto
14. - **COSA E' UN "INTERNET-BROWSER"?** Un programma Client per navigare in Internet
15. - **COSA E' UN "LINK"?** Un collegamento ipertestuale
16. - **COSA E' UN "SERVER"?** Una componente informatica che fornisce servizi ad altre componenti attraverso una rete
17. - **COSA E' UN "TROJAN HORSE"?** Un programma che nasconde il suo vero scopo
18. - **COSA E' UNA LAN?** Un'architettura di rete di tipo client-server
19. - **COSA SI INTENDE CON IL TERMINE JAVA?** Un linguaggio di programmazione
20. - **COSA SI INTENDE CON IL TERMINE LOGIN?** Procedura di ingresso

FONDAZIONE I.R.C.C.S. POLICLINICO SAN MATTEO PAVIA

ALLEGATO 13

RASopathies for Radiologists

Atsuhiko Handa, MD • Yuko Tsujioka, MD* • Gen Nishimura, MD, PhD • Taiki Nozaki, MD, PhD • Tatsuo Kono, MD, PhD • Masahiro Jinzaki, MD, PhD*
Taylor Harms, MD • Susan A. Connolly, MD • Takashi Shawn Sato, MD • Yutaka Sato, MD, PhD

* A.H. and Y.T. contributed equally to this work.
Author affiliations, funding, and conflicts of interest are listed at the end of this article.

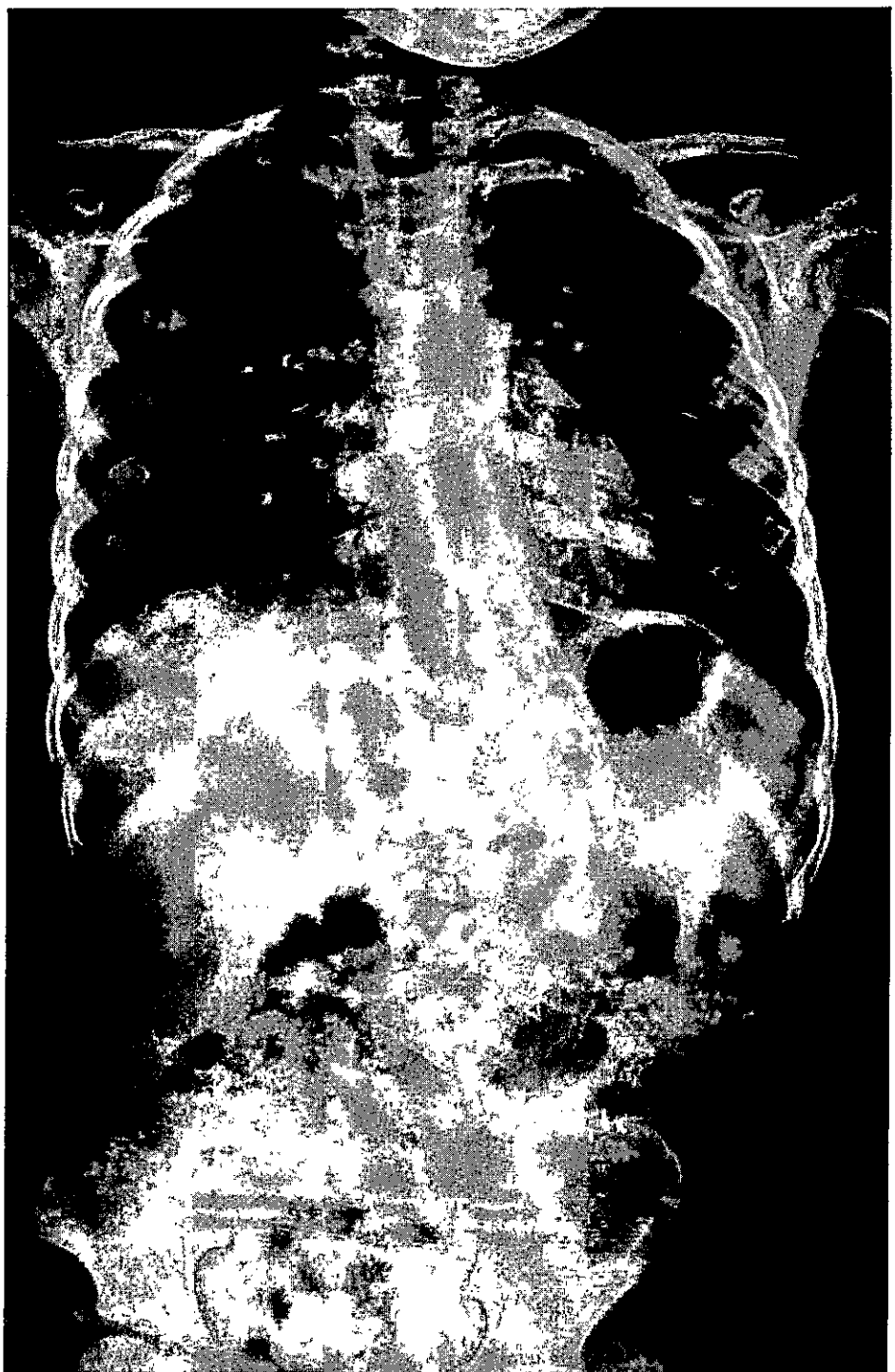

RASopathies are a heterogeneous group of genetic syndromes caused by germline mutations in a group of genes that encode components or regulators of the Ras/mitogen-activated protein kinase (MAPK) signaling pathway. RASopathies include neurofibromatosis type 1, Legius syndrome, Noonan syndrome, Costello syndrome, cardiofaciocutaneous syndrome, central conducting lymphatic anomaly, and capillary malformation–arteriovenous malformation syndrome. These disorders are grouped together as RASopathies based on our current understanding of the Ras/MAPK pathway. Abnormal activation of the Ras/MAPK pathway plays a major role in development of RASopathies. The individual disorders of RASopathies are rare, but collectively they are the most common genetic condition (one in 1000 newborns). Activation or dysregulation of the common Ras/MAPK pathway gives rise to overlapping clinical features of RASopathies, involving the cardiovascular, lymphatic, musculoskeletal, cutaneous, and central nervous systems. At the same time, there is much phenotypic variability in this group of disorders. Benign and malignant tumors are associated with certain disorders. Recently, many institutions have established multidisciplinary RASopathy clinics to address unique therapeutic challenges for patients with RASopathies. Medications developed for Ras/MAPK pathway–related cancer treatment may also control the clinical symptoms due to an abnormal Ras/MAPK pathway in RASopathies. Therefore, radiologists need to be aware of the concept of RASopathies to participate in multidisciplinary care. As with the clinical manifestations, imaging features of RASopathies are overlapping and at the same time diverse. As an introduction to the concept of RASopathies, the authors present major representative RASopathies, with emphasis on their imaging similarities and differences.

RG

PEDIATRIC IMAGING

TestYour Knowledge

CME

RadioGraphics 2024; 44(5):e230153
https://doi.org/10.1148/rg.230153

Content Codes: CT, MR, PD

Abbreviations: CCLA = central conducting lymphatic anomaly, CFC = cardiofaciocutaneous, CM-AVM = capillary malformation–arteriovenous malformation, MAPK = mitogen-activated protein kinase, NF1 = neurofibromatosis type 1

TEACHING POINTS

- RASopathies are a heterogeneous group of genetic syndromes caused by germline mutations in a group of genes that encode components or regulators of the Ras/mitogen-activated protein kinase (MAPK) signaling pathway.
- RASopathies include neurofibromatosis type 1 (NF1), Legius syndrome, Noonan syndrome, Noonan syndrome with multiple lentigines, Costello syndrome, cardiofaciocutaneous (CFC) syndrome, central conducting lymphatic anomaly (CCLA), and capillary malformation–arteriovenous malformation (CM-AVM) syndrome.
- Activation or dysregulation of the common Ras/MAPK pathway gives rise to overlapping clinical features of RASopathies, involving the cardiovascular, lymphatic, musculoskeletal, cutaneous, and central nervous systems.
- The imaging features of RASopathies are overlapping and at the same time diverse.
- It may be possible to use modulators for the Ras/MAPK pathway to alleviate some of the complications seen in RASopathies.

Introduction

RASopathies are a heterogeneous group of genetic syndromes caused by germline mutations in a group of genes that encode components or regulators of the Ras/mitogen-activated protein kinase (MAPK) signaling pathway. This pathway is important in passing signals from cellular surface receptors to the DNA in the nucleus of the cell and plays an important role in regulating the cell cycle and cellular growth, differentiation, and survival (1,2). RASopathies include neurofibromatosis type 1 (NF1), Legius syndrome, Noonan syndrome, Noonan syndrome with multiple lentigines, Costello syndrome, cardiofaciocutaneous (CFC) syndrome, central conducting lymphatic anomaly (CCLA), and capillary malformation–arteriovenous malformation (CM-AVM) syndrome.

These disorders are grouped together as RASopathies based on our current understanding of the Ras/MAPK pathway (Fig 1). Abnormal activation or dysregulation of the Ras/MAPK pathway plays a major role in development of RASopathies. The individual disorders of RASopathies are rare, but collectively they are the most common genetic condition (one in 1000 newborns).

Activation or dysregulation of the common Ras/MAPK pathway gives rise to overlapping clinical features of RASopathies, involving the cardiovascular, lymphatic, musculoskeletal, cutaneous, and central nervous systems (Table 1) (1,3). Phenotypically, patients with RASopathies show craniofacial features similar to those seen in Noonan syndrome. Feeding difficulties, failure to thrive, short stature, as well as neurocognitive and behavioral issues are also common in RASopathies.

Benign and malignant tumors are associated with certain disorders (Table 2). At the same time, there is much phenotypic variability in this group of disorders—the reasons behind it remain largely unknown. Perhaps more complex control mechanisms are hidden behind the major pathway, for example, cross talk with other signaling pathways and the tissue specificity of each signaling molecule. On the basis of clinical similarities and variabilities, molecular diagnosis is essential.

Recently, many institutions have established multidisciplinary RASopathy clinics to address unique therapeutic challenges for patients with RASopathies. Medications developed for Ras/MAPK pathway–related cancer treatment may also control an abnormal Ras/MAPK pathway and alleviate the clinical symptoms in RASopathies. Therefore, radiologists need to be aware of the concept of RASopathies to participate in multidisciplinary care.

As with the clinical manifestations, the imaging features of RASopathies are overlapping and at the same time diverse. As an introduction to the concept of RASopathies, we present major representative RASopathies, with emphasis on their imaging similarities and differences. The imaging strategy should be tailored according to the patient's provisional diagnosis and clinical questions.

Neurofibromatosis Type 1

NF1 is an autosomal dominant disorder and was the first syndrome identified as being caused by mutation of a gene in the Ras/MAPK pathway (4–8). It affects one in 3000 live births. It is caused by heterozygous loss of function mutation of the *NF1* gene, which encodes tumor suppressor protein neurofibromin 1. Inactivation of neurofibromin 1 causes prolonged activation of RAS proteins or the cyclic adenosine monophosphate (AMP) pathway, resulting in an overall increase in active guanosine triphosphate (GTP)–bound Ras. Approximately half of patients with NF1 have NF1 mutations transmitted from a parent, while the remaining half have de novo mutations (9).

Major clinical symptoms of NF1 include café-au-lait macules, axillary and inguinal freckling, Lisch nodules of the iris, and cutaneous neurofibromas. Patients also show a predisposition to developing certain malignancies, with cancer risk 2.5 times higher than that of the general population (10).

Neurofibromas

Neurofibromas or benign peripheral nerve sheath tumors are the hallmark of NF1. They can be localized, diffuse (infiltrative), or plexiform (11). Plexiform neurofibromas, which are tortuous expansions of a long nerve segment and its branches with transspatial extension, are essentially pathognomonic for NF1 (Fig 2). They can occur in up to 40% of patients with NF1 and tend to occur multifocally. Malignant transformation to malignant peripheral nerve sheath tumors may occur from any variety of neurofibroma, but particularly from plexiform neurofibromas (Fig 3). It is the most common malignancy found in patients with NF1.

Imaging criteria are not necessarily reliable in differentiating benign from malignant neurofibroma. Findings favoring malignant transformation include pain, rapid growth, large

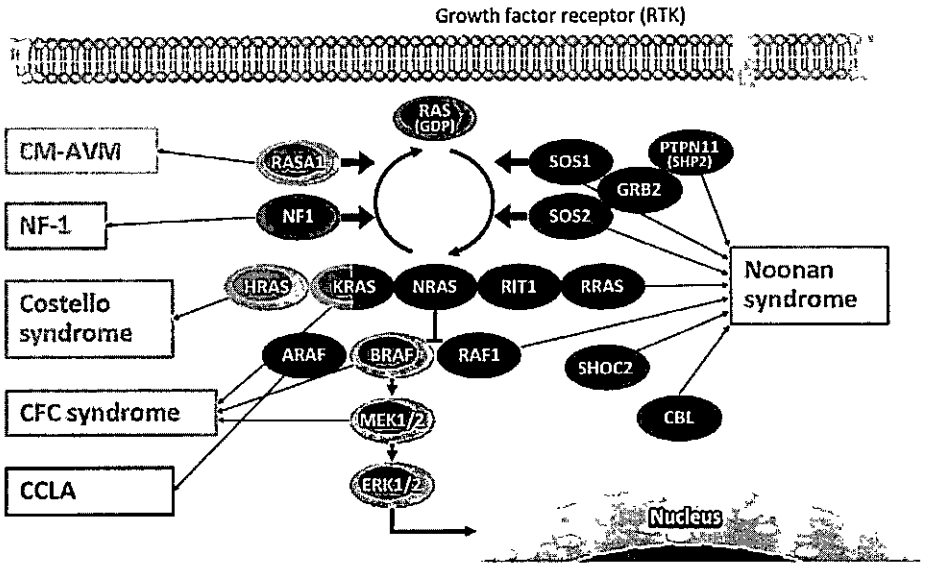

Figure 1. RAS cascade. NF1, Noonan syndrome, Costello syndrome, CFC syndrome, CCLA, and CM-AVM syndrome are grouped together as RASopathies based on the common molecular thread of the Ras/MAPK pathway. RAS proteins are small guanosine triphosphate (GTP)–binding proteins that function as biologic switches at the cell surface. When activated, RAS-GTP triggers the Ras/MAPK signaling cascade, which regulates the cell cycle and cellular growth, differentiation, and survival. Somatic mutations in the Ras/MAPK pathway have been known to cause many types of cancer. Molecular inhibition of this pathway have shown promise in treatment development. Germline mutations in the Ras/MAPK pathway can cause classic genetic disorders (RASopathies), as listed above. Since RASopathies have germline Ras/MAPK pathway dysregulation, they may be amenable to treatment with pathway modulators that were originally developed for cancer treatment. *GDP* = guanosine diphosphate, *RTK* = receptor tyrosine kinase.

size, peripheral enhancement pattern, perilesional edema, cystic changes, and heterogeneity on T1-weighted images. Fluorodeoxyglucose (FDG) PET is also useful for identifying malignant transformation, which demonstrates substantially higher standardized uptake value (SUV) compared with that of benign neurofibromas.

Vascular Complications

Vasculopathies associated with NF1 are variable and often asymptomatic (12). They involve different-sized vessels, ranging from small arterioles to the aorta. Among the NF1-related vasculopathies, renal artery stenosis is the most important and is commonly symptomatic (eg, hypertension) in the pediatric age group (Fig 4); it can be categorized as part of middle aortic syndrome. Middle aortic syndrome is characterized by segmental or diffuse narrowing of the abdominal aorta with ostial stenosis of its major branches (Fig 5) (13). It has been proposed that vasculopathy associated with NF1 results from abnormal neurofibromin function that leads to excessive proliferation of vascular smooth muscle cells, causing luminal narrowing.

NF1 is the most common genetic disorder associated with middle aortic syndrome. Therefore, annual blood pressure monitoring is recommended, and persistent hypertension requires assessment of large vessels, including renal arteries (7). CT angiography or MR angiography can help further characterize these vessels. Renal artery stenosis associated with NF1 (as part of middle aortic syndrome) is usually ostial in location, compared with fibromuscular dysplasia, where 95% of all stenotic segments are found in the distal two-thirds of the renal artery with a string-of-pearls appearance (14).

Congenital heart disease occurs more commonly (~2%) in patients with NF1 than in the general population (12,15). Pulmonary valve stenosis is by far the most common congenital heart defect seen in NF1. Other cardiac malformations seen in NF1 include atrial septal defect, ventricular septal defect, aortic coarctation, tetralogy of Fallot, mitral valve prolapse, and hypertrophic cardiomyopathy.

Pulmonary Complications

NF1 is associated with diffuse lung disease in 10%–20% of patients, typically manifesting with upper-lobe cystic and bullous disease and with basilar interstitial lung disease (Fig 6), although it is not considered pathognomonic (16). This can be early onset and seen in children with NF1 (17). This pulmonary parenchymal disease is generally attributed to a mesenchymal defect, resulting in primary deposition of collagen in the alveolar wall (18). Pulmonary hypertension is a rare complication of NF1 and is thought to be secondary to parenchymal lung disease or primary vascular disease (Fig 7).

Skeletal Complications

Congenital tibial dysplasia is characterized by apex anterolateral bowing of the tibia commonly concurrent with bowing of

Table 1: RASopathies with Clinical, Cardiovascular, and Musculoskeletal Features

RASopathy	Clinical Features	Cardiovascular Features	Musculoskeletal Features
NF1	Café-au-lait macules Intertriginous freckling Neurofibromas Lisch nodules Optic glioma Mild neurocognitive impairment Cancer predisposition	Pulmonary valve stenosis	Short stature Pectus carinatum or excavatum Scoliosis Vertebral anomalies Congenital tibial dysplasia Low BMD or osteoporosis
Noonan syndrome	Distinct facial features (ocular hypertelorism, ptosis, downslanting palpebral fissures) Mild intellectual disability Delayed puberty, hypogonadism Bleeding disorders Cancer predisposition	Congenital heart disease (pulmonary valve stenosis, septal defects, and HCM)	Short stature Pectus carinatum or excavatum Scoliosis or kyphosis Vertebral anomalies Cubitus valgus Brachydactyly Micrognathia Low BMD Giant cell lesions
Costello syndrome	Distinct facial features Dermatologic features Postnatal growth delay Cutaneous papillomas Cancer predisposition	Congenital heart disease (HCM and pulmonary valve stenosis)	Short stature Chest wall anomalies Scoliosis or kyphosis Hip dysplasia Joint laxity (small joints) Joint contractures (large joints) Tight heel cords Low BMD
CFC syndrome	Facial features of Noonan syndrome Ocular abnormalities Failure to thrive; gastrointestinal dysfunction Cutaneous abnormalities	Congenital heart disease (pulmonary valve stenosis, HCM, and septal defects)	Short stature Pectus carinatum or excavatum Scoliosis or kyphosis Joint hyperextensibility or contractures Pes planus Clinodactyly or syndactyly Hypotonia or myopathy Low BMD
CM-AVM syndrome	Multifocal capillary malformations and fast-flow vascular lesions	Cardiovascular malformations	Leg length discrepancies or limb overgrowth related to vascular limb lesions

Source.—Reference 3.
Note.—BMD = bone mineral density, HCM = hypertrophic cardiomyopathy.

the fibula at the junction of the middle to distal thirds of the lower leg, which may be complicated by fracture or pseudarthrosis in severe cases (Fig 8) (19). Approximately 3%–4% of children with NF1 show congenital tibial dysplasia. Conversely, approximately 40%–90% of children with congenital tibial dysplasia are later diagnosed with NF1 (20).

Congenital tibial dysplasia can be the first manifestation of NF1. Its presence should raise suspicion for NF1, even if affected individuals do not have other features of NF1. Histologically, fibrous tissue instead of neurofibroma is seen at the site of bowing. The anterolateral bowing in congenital tibial dysplasia should not be confused with the benign congenital posteromedial bowing seen secondary to abnormal intrauterine positioning.

Spinal abnormalities are seen in up to one-third of patients with NF1, leading to scoliosis (19). Scoliosis in NF1 can be either idiopathic-like (more common; without spinal dysplastic changes) or secondary (also called dystrophic; with spinal dysplastic changes). Dystrophic scoliosis tends to manifest in preadolescent children as short-segment (four to six vertebrae) sharply angulated curvature, often with vertebral wedging, vertebral scalloping, spinal canal widening, defective pedicles, or rib penciling (Fig 9) (21). These findings can be caused by paraspinal neurofibromas, meningoceles, or dural ectasia associated with NF1, which can be best assessed at MRI, although these dysplastic changes may develop in the setting of normal spinal contents without focal lesions (mesodermal dysplasia). It is important to recognize dystrophic scoliosis because it tends to evolve more rapidly into severe curvature and require earlier surgical intervention when compared with idiopathic scoliosis.

Rib abnormalities in NF1 include well-defined erosions of one or more ribs, which may cause the classic ribbon rib deformity, with thinned and wavy ribs in severe cases (Fig 10) (22). This deformity may be secondary to either neurofibroma-induced osseous remodeling or primary mesodermal dysplasia, as with spinal dysplasia in NF1.

Table 2: Tumors Associated with RASopathies

RASopathy	Genes	Associated Malignancies
NF1	*NF1*	Glioma Rhabdomyosarcoma Malignant peripheral nerve sheath tumor JMML Breast cancer Gastrointestinal cancers (eg, GIST)
Noonan syndrome	*PTPN11* *SOS1* *RAF1* *RIT1* *KRAS* *CBL* *SOS2* *NRAS* *SHOC2* *RRAS* *LZTR1* *BRAF*	JMML Neuroblastoma Acute lymphocytic leukemia Glioma Rhabdomyosarcoma Acute myelogenous leukemia Testicular cancer Non-Hodgkin lymphoma Colon cancer
Costello syndrome	*HRAS*	Rhabdomyosarcoma Neuroblastoma Bladder cancer (transitional cell carcinoma)
CFC syndrome	*BRAF* *MAP2K1* *MAP2K2* *KRAS* *SHOC2*	…
CM-AVM syndrome	*RASA1*	…

Source.—Reference 10.
Note.—GIST = gastrointestinal stromal tumor, JMML = juvenile myelomonocytic leukemia.

Polyostotic nonossifying fibromas are a rare association of NF1. Radiographs are usually diagnostic, and findings include a well-defined, cortical-based, lytic lesion with sclerotic margins and endosteal scalloping, most commonly around the knee (Fig 11). Multiple large nonossifying fibromas with thinning of the cortex are at high risk of pathologic fractures.

A combination of multiple nonosssifying fibromas with café-au-lait macules but not with neurofibromas has been known as Jaffe-Campanacci syndrome (23). Jaffe-Campanacci syndrome was once considered a separate entity from NF1; however, there has been growing evidence that it may be a subtype of NF1 (23). Recent research has found somatic mutations activating the Ras/MAPK pathway (KRAS and NF1) in ~80% of nonossifying fibromas (24). These findings indicate that nonossifying fibromas, long considered to be reactive, should be considered a true neoplasm.

Sphenoid wing dysplasia, a defect of the posterosuperior orbital wall, is a characteristic finding seen in approximately 10% of patients with NF1 (Fig 12) (25). This is associated with adjacent plexiform neurofibromas or mesodermal dysplasia (26). Herniation of intracranial contents through the defect can result in pulsating exophthalmos.

Childhood osteoporosis is frequent in NF1, and affected children may be at slightly increased risk for fractures. However, there are no clinical trials to support the use of osteoporotic drugs (19).

Central Nervous System Complications

Focal areas of signal intensity (FASIs), also called unidentified bright objects, are hyperintense areas on T2-weighted images commonly seen in the basal ganglia, thalamus, corpus callosum, cerebral white matter, brainstem, and cerebellum in children with NF1 (Fig 13) (27). This is the most common central nervous system abnormality seen with NF1 (60%–70%). FASIs are considered a benign process caused by increased fluid accumulation in intramyelin vacuoles without inflammatory changes or demyelination. FASIs appear during infancy, increase in number and size to a peak at around age 7 years, then spontaneously regress by adulthood.

Children with NF1 (especially those <6 years of age) are at risk for optic pathway gliomas (28). Approximately 20% of patients with NF1 will develop optic pathway gliomas. These children may be asymptomatic or present with reduced visual acuity. The majority of these tumors are World Health Organization (WHO) grade I tumors (pilocytic astrocytoma), show a favorable course compared with that of sporadic optic pathway gliomas, and in some cases regress spontaneously.

Bilateral optic pathway gliomas are almost pathognomonic for NF1 (Fig 14). After the optic pathway, the brainstem is the second most common location of brain tumors. Higher-grade gliomas can be seen, including glioblastoma multiforme (Fig 15).

Dural ectasia is progressive focal dilatation of the dural sac (Fig 16) (29). Imaging findings include vertebral body scalloping and erosion, pedicle erosion, and neuroforaminal enlargement. The pathogenesis of dural ectasia in NF1 is likely secondary to infiltration of neurofibromas into dural tissues, leading to focal dural weakening and subsequent ectasia. The majority of ectasias are in close proximity to plexiform neurofibromas.

As with vascular involvement of the renal arteries, NF1 may involve the intracranial arteries as well (30). Moyamoya syndrome is a progressive cerebral arteriopathy with increased incidence in children with NF1 (Fig 17) (31). It manifests as steno-occlusive disease of the intracranial arteries, resulting in collateral vessel formation that causes a characteristic "puff of smoke" appearance. Most patients are asymptomatic, although there are patients (<4 years of age) who present with an aggressive form of moyamoya syndrome.

Children with NF1 have an increased risk of leukemia (the relative risk for acute lymphocytic leukemia is 5.4) (32). The cumulative risk of malignancy by age 50 years in patients with NF1 has been estimated to be 20%–39%, with a lifetime cancer risk of around 60%. Patients with NF1 have exceptionally high risks for malignant brain tumors (around a 40-fold risk of high-grade glioma) and endocrine cancers (an over 74-fold increased risk for adrenal cancer). In addition, patients with NF1 have an over 1000-fold increased risk for malignant peripheral nerve sheath tumor.

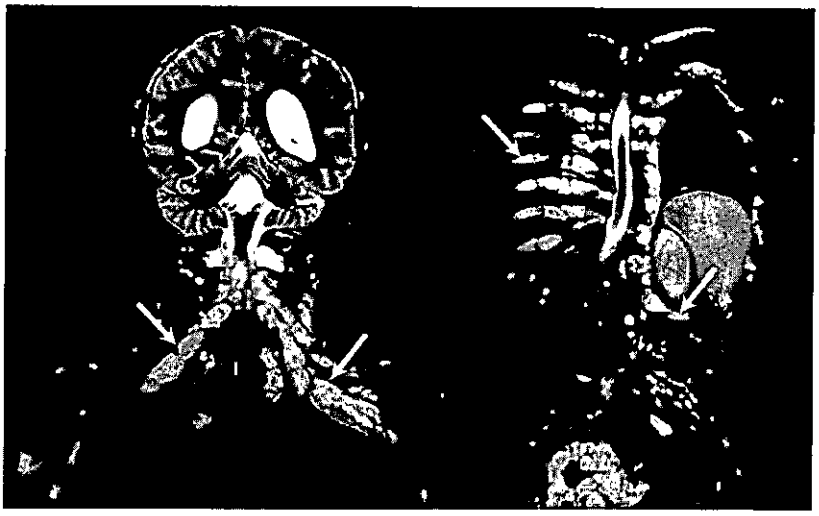

Figure 2. Plexiform neurofibromas in a 15-year-old boy with NF1. Coronal T2-weighted MR images of the head, neck, and chest show multiple T2-hyperintense plexiform expansions of a long nerve segment and its branches (arrows), compatible with plexiform neurofibromas.

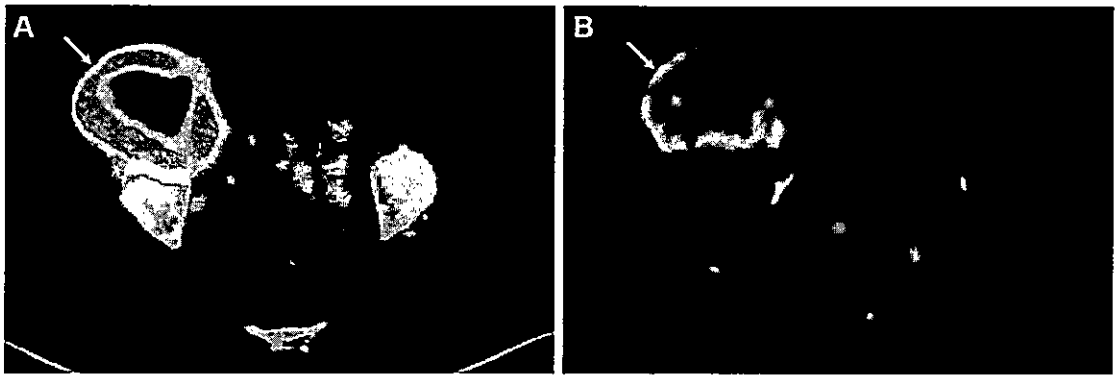

Figure 3. Malignant peripheral nerve sheath tumor involving the right inguinal region in a 48-year-old woman with NF1 who presented with worsening right inguinal pain. **(A)** Axial fluorodeoxyglucose (FDG) PET/CT image shows a large mass in the right inguinal region with FDG avidity (arrow). **(B)** Axial diffusion-weighted image shows the mass with reduced diffusivity, predominantly along the periphery of the mass (arrow). (Apparent diffusion coefficient [ADC] map not shown.)

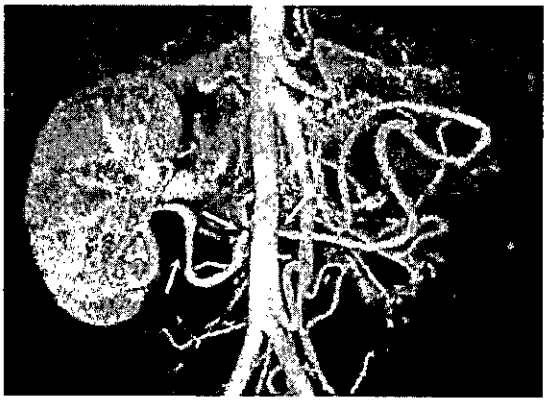

Figure 4. Renal artery stenosis in a child with NF1. MR angiogram of the abdomen shows moderate to severe narrowing (arrows) of the bilateral renal artery ostia as well as the midportion of the right renal artery.

Legius Syndrome

Legius syndrome is characterized by multiple café-au-lait macules resembling those of NF1, but without neurofibromas or other tumor manifestations of NF1. Additional clinical manifestations include intertriginous freckling, lipomas, macrocephaly, and developmental delays. It is caused by *SPREDI* mutations.

Noonan Syndrome

Noonan syndrome is a predominantly autosomal dominant disorder (33,34) affecting one in 1000–2000 live births. It is caused by heterozygous de novo mutations (60%) in the genes of the Ras/MAPK pathway. The majority of cases (>50%) are due to mutations in *PTPN11*, which lead to increased signaling of the Ras/MAPK pathway (35) and are highly associated with pulmonary artery stenosis. *RAF1* mutations are associated with hypertrophic cardiomyopathy (95%) and negatively associated with pulmonary valve stenosis (36,37). Noonan syndrome is also caused by mutations in other genes, including *SOS1*, *KRAS*, *NRAS*, *SHOC2*, and *CBL* (1).

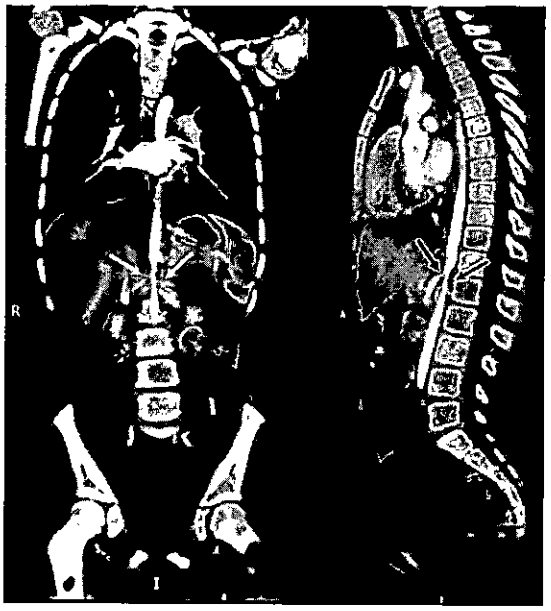

Figure 5. Middle aortic syndrome in a 9-year-old girl with NF1 and hypertension. Coronal (left) and sagittal (right) CT angiograms of the chest, abdomen, and pelvis show moderate to severe narrowing of the mid aorta (blue arrow), bilateral renal artery ostia (white arrows), and superior mesenteric artery (SMA) ostium (black arrow).

Figure 6. Interstitial lung disease in a 26-year-old woman with NF1. Axial CT images of the chest at different levels show peripheral interlobular septal thickening (arrows) in the bibasilar lungs.

The major clinical symptoms of Noonan syndrome include distinctive craniofacial abnormalities, pterygium colli (webbed neck), short stature, neurocognitive disability (such as learning disability) and behavioral issues, and cryptorchidism. Fetal US may show increased nuchal thickness, cystic

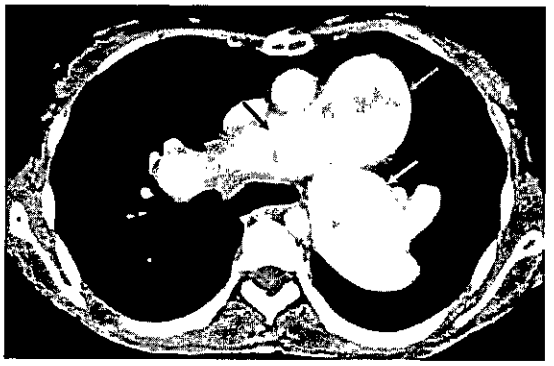

Figure 7. Pulmonary hypertension in a child with NF1. Axial CT image of the chest with intravenous contrast material shows marked dilatation of the main (red arrow), right (black arrow), and left (white arrow) pulmonary arteries as a consequence of long-standing pulmonary hypertension.

hygroma, hydrops, pleural effusions, ascites, and polyhydramnios (Fig 18) (38). Pterygium colli represents a late consequence of nuchal lymphedema. Multiple coagulation-factor deficiencies and platelet dysfunction are also prevalent. Although the bleeding disorders are mostly subclinical, Noonan syndrome may rarely be associated with hemorrhagic crisis, particularly in the perioperative period.

Congenital heart disease is present in up to 80% of patients with Noonan syndrome, with pulmonary valve stenosis being the most common form (up to 40%) (39). Other congenital heart abnormalities include septal defects (up to 10%), such as atrial septal defect, ventricular septal defect, and atrioventricular septal defect. Hypertrophic cardiomyopathy is also common (Fig 19) (up to 20%), and more severe cardiac involvement correlates with lower survival rates (40).

Many patients with Noonan syndrome have lymphatic disease such as lymphedema, pleural effusion, pericardial effusion, ascites, and protein-losing enteropathy (41). These are most likely associated with CCLA, causing retrograde intercostal flow, pulmonary lymphatic perfusion, and thoracic duct abnormalities (42). It is even possible that CCLA may be present in essentially all patients with Noonan syndrome, manifesting as merely subclinical lymphedema in mild cases (Fig 20) (43).

Skeletal abnormalities in patients with Noonan syndrome include scoliosis and characteristic pectus deformity of the chest, which is seen in most patients, with pectus carinatum superiorly and pectus excavatum inferiorly (33). Multiple giant cell lesions, particularly of the jaw, are often seen in patients with Noonan syndrome (Fig 21).

Patients with Noonan syndrome have a slightly increased risk (4%) of developing malignancy with the cumulative risk for cancer by age 20 years (Table 1) (44). Although the most common cancers include central nervous system tumors, neuroblastoma, acute lymphoblastic leukemia, and rhabdomyosarcoma, children with Noonan syndrome are predisposed to juvenile myelomonocytic leukemia (JMML)–like myeloproliferative disorders (Fig 22) (45). JMML is a unique hematopoietic disorder, with a manifestation ranging from the neonate to early childhood, and can be fatal in sporadic

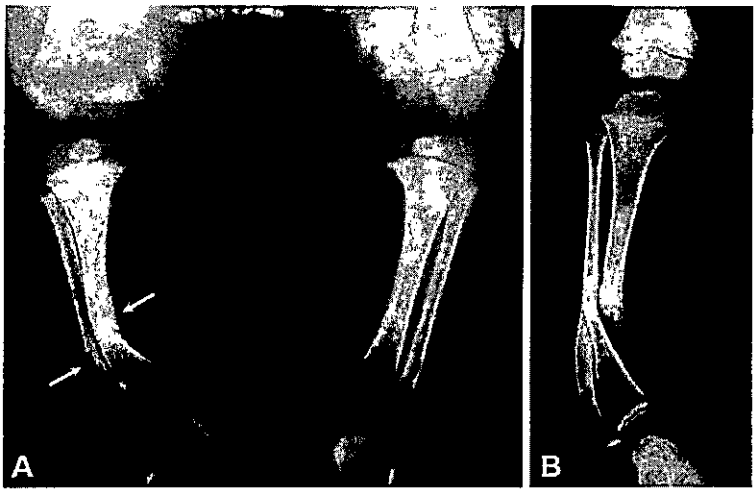

Figure 8. Congenital tibial dysplasia in a child with NF1. **(A)** Frontal radiograph of the bilateral legs at 1 month of age shows apex anterolateral angulation of the distal shafts of the tibia and fibula on the right (arrows) with medial cortical thickening. **(B)** Frontal radiograph of the right leg at 3 years of age shows pseudarthrosis of the mid to distal tibia and distal fibular bowing.

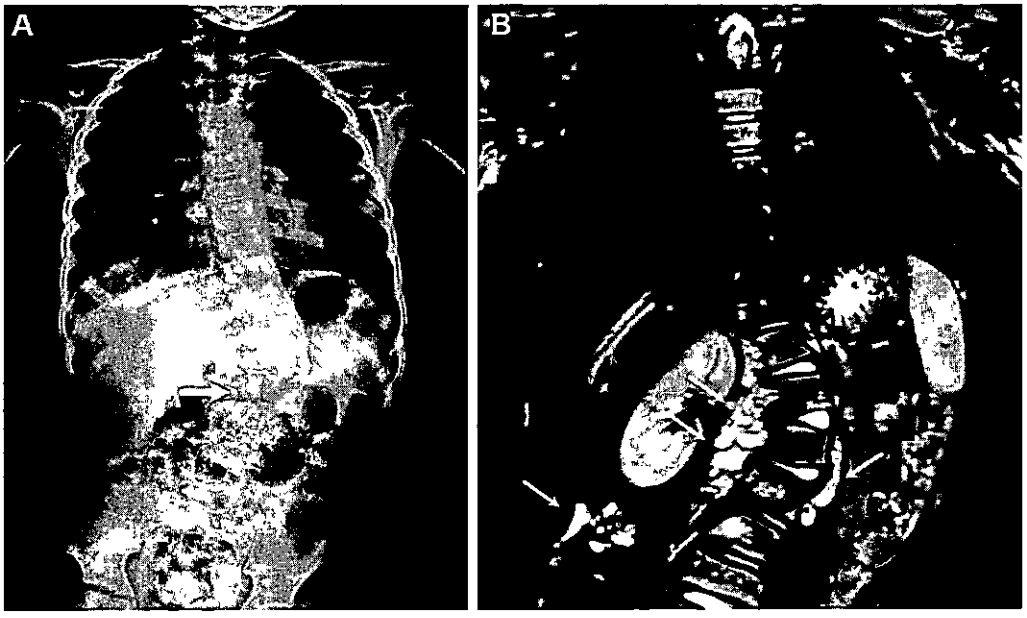

Figure 9. Dystrophic scoliosis due to paraspinal neurofibromas in a 6-year-old boy with NF1. **(A)** Frontal radiograph of the spine shows short-segment levoconvex scoliosis of the lumbar spine (arrow). **(B)** Coronal T2-weighted MR image of the spine shows multiple neurofibromas (arrows), predominantly in the right paraspinal region, causing scoliosis. There are smaller neurofibromas in the left paraspinal region and the right-sided pelvis as well.

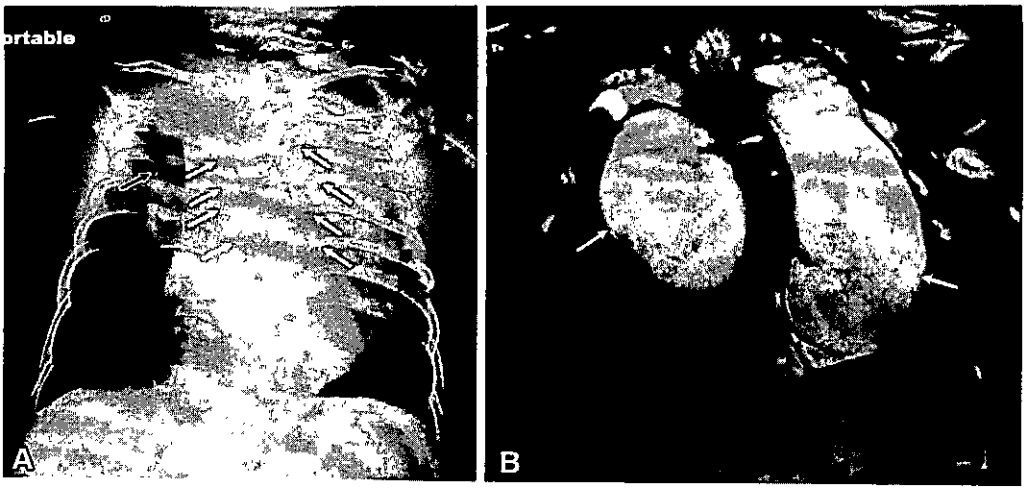

Figure 10. Ribbon rib deformity in a 3-year-old girl with NF1. **(A)** Frontal chest radiograph shows thinned and wavy ribs (white arrows) in the proximal aspect of the ribs, along with an enlarged mediastinal silhouette (black arrow). A superior vena cava (SVC) stent is also noted. **(B)** Coronal T2-weighted MR image shows massive paraspinal plexiform neurofibromas (arrows).

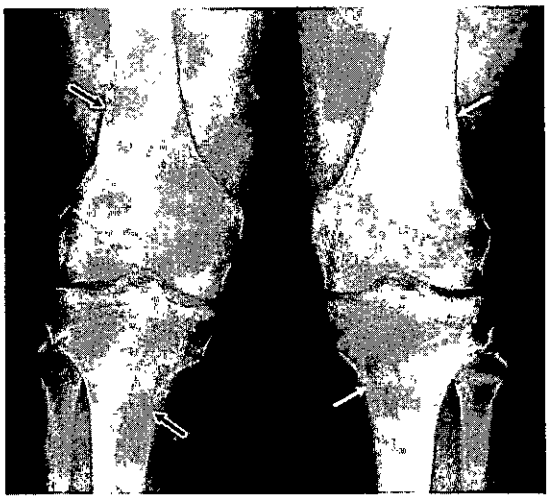

Figure 11. Multiple nonossifying fibromas in a 15-year-old boy with NF1. Frontal radiograph of the bilateral knees shows multiple well-defined, cortical-based, lytic lesions (arrows) with sclerotic margins in the distal femora and proximal tibias. The right distal femoral and proximal tibial lesions also show internal sclerosis related to curettage and allograft bone grafting to decrease the risk for pathologic fracture. The same surgery was performed on the left-sided distal femoral and proximal tibial lesions after this study.

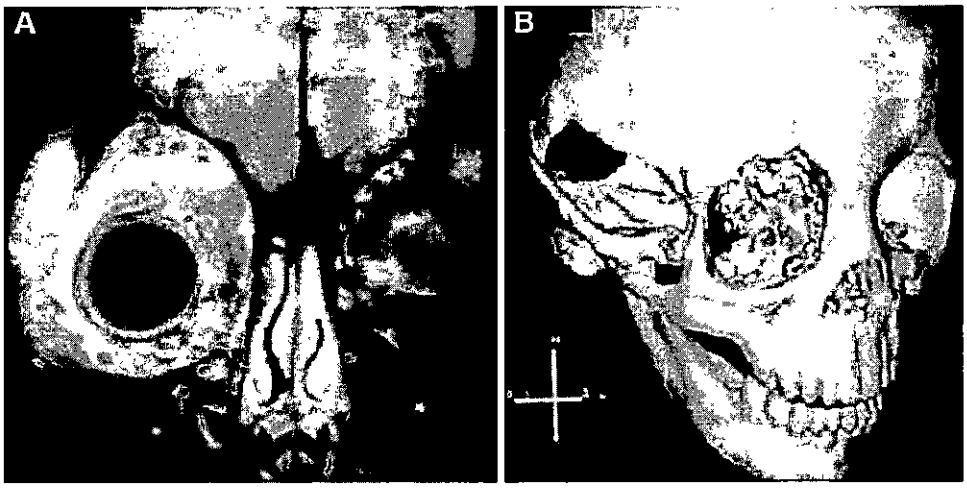

Figure 12. Sphenoid wing dysplasia in a 4-year-old girl with NF1 and plexiform neurofibromas. **(A)** Coronal contrast-enhanced T1-weighted MR image shows massive, contrast-enhancing, transspatial plexiform neurofibromas in the right orbit, leading to sphenoid wing dysplasia. Note the marked exophthalmos. **(B)** Three-dimensional rendering of the face shows erosive changes of the sphenoid wing and enlargement of the orbit.

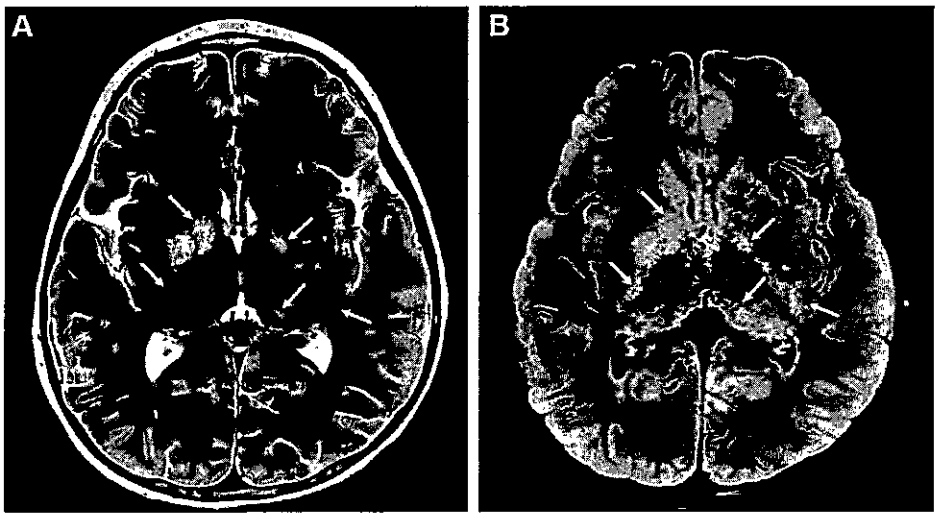

Figure 13. Focal areas of signal intensity (FASIs) in a 4-year-old girl with NF1. Axial T2-weighted **(A)** and fluid-attenuated inversion-recovery (FLAIR) **(B)** MR images of the brain show areas of increased signal intensity (arrows) in the basal ganglia, thalamus, internal capsule, and cerebral white matter. There was no enhancement on a contrast-enhanced image (not shown).

cases. Interestingly, JMML occurring in patients with Noonan syndrome is often benign and transitory and may regress without treatment.

Noonan Syndrome with Multiple Lentigines

Noonan syndrome with multiple lentigines (formerly lentigines [multiple], electrocardiographic abnormalities, ocular

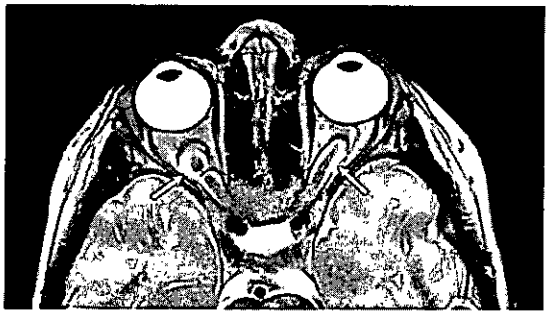

Figure 14. Bilateral optic pathway gliomas in a 4-year-old girl with NF1 (same patient as in Fig 12). Axial MR image shows bilateral T2-hyperintense masses (arrows) with thin hypointense rims along the bilateral optic nerves, consistent with optic pathway gliomas.

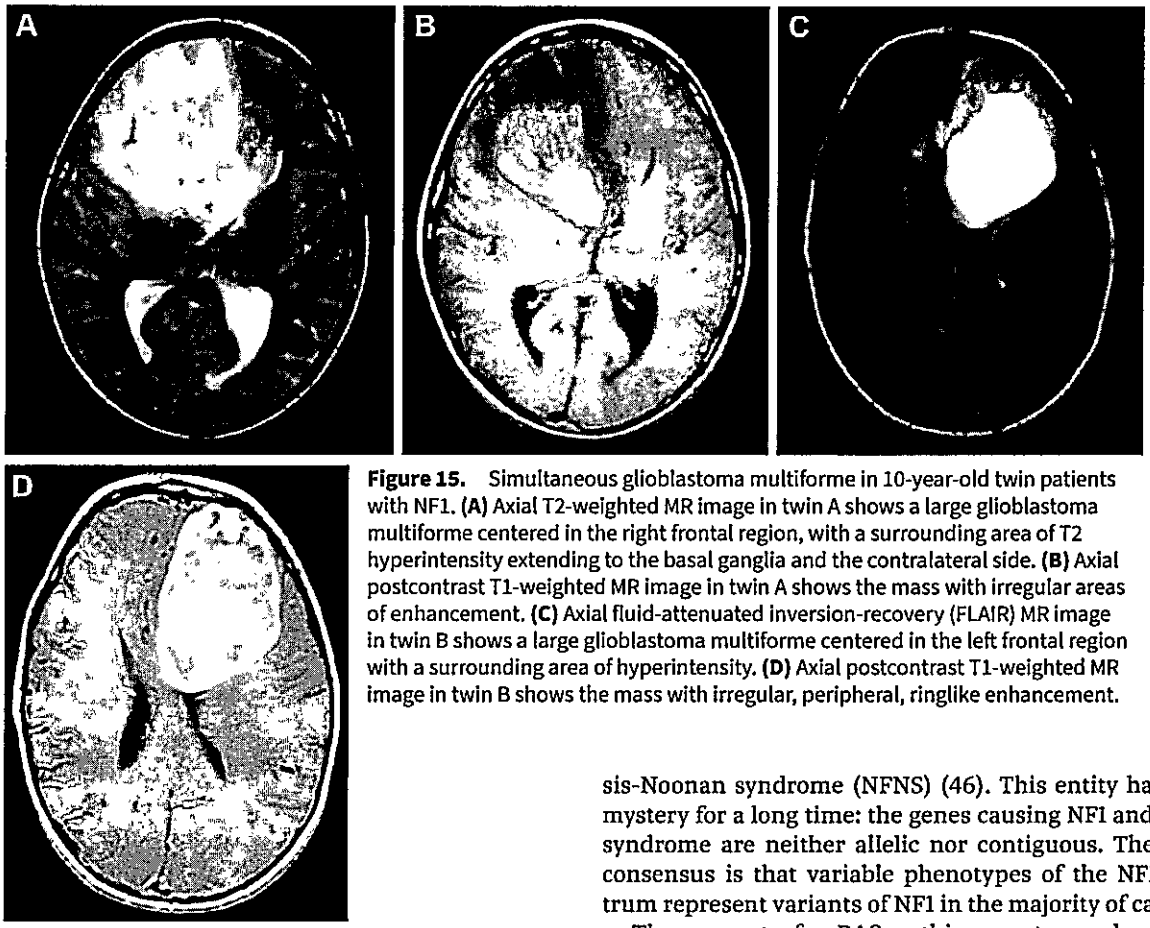

Figure 15. Simultaneous glioblastoma multiforme in 10-year-old twin patients with NF1. **(A)** Axial T2-weighted MR image in twin A shows a large glioblastoma multiforme centered in the right frontal region, with a surrounding area of T2 hyperintensity extending to the basal ganglia and the contralateral side. **(B)** Axial postcontrast T1-weighted MR image in twin A shows the mass with irregular areas of enhancement. **(C)** Axial fluid-attenuated inversion-recovery (FLAIR) MR image in twin B shows a large glioblastoma multiforme centered in the left frontal region with a surrounding area of hyperintensity. **(D)** Axial postcontrast T1-weighted MR image in twin B shows the mass with irregular, peripheral, ringlike enhancement.

hypertelorism, *p*ulmonary stenosis, *a*bnormal genitalia, *r*etardation of growth, and *d*eafness [sensorineural] [LEOPARD] syndrome) is a distinctive condition with similar craniofacial dysmorphic features as in Noonan syndrome, but patients also have multiple skin lentigines. Similar to Noonan syndrome, Noonan syndrome with multiple lentigines is associated with mutations in *PTPN11*, *RAF1*, and rarely *BRAF*.

Overlapping Phenotypes of NF1 and Noonan Syndrome

There are many patients who show clinical features of both NF1 and Noonan syndrome, often termed neurofibromatosis-Noonan syndrome (NFNS) (46). This entity has been a mystery for a long time: the genes causing NF1 and Noonan syndrome are neither allelic nor contiguous. The current consensus is that variable phenotypes of the NFNS spectrum represent variants of NF1 in the majority of cases (47).

The concept of a RASopathies spectrum also explains the overlap between other seemingly disparate diseases. An example is a subset of patients with multiple giant cell lesions in the mandible and maxilla with clinical features like those of Noonan syndrome. Initially, this manifestation was considered to be merely a Noonan syndrome–like disorder (Noonan-like/multiple giant cell lesion syndrome) independent of classic Noonan syndrome; however, genetic analyses confirmed that the disorder is part of a spectrum seen in patients with Noonan syndrome (48).

Another example is Jaffe-Campanacci syndrome. This disorder, now recognized as a variation of NF1, is not only associated with multiple nonossifying fibromas but can also be complicated by cherubism-like multiple osteolytic lesions of the maxillofacial bones (Fig 23). On the basis of

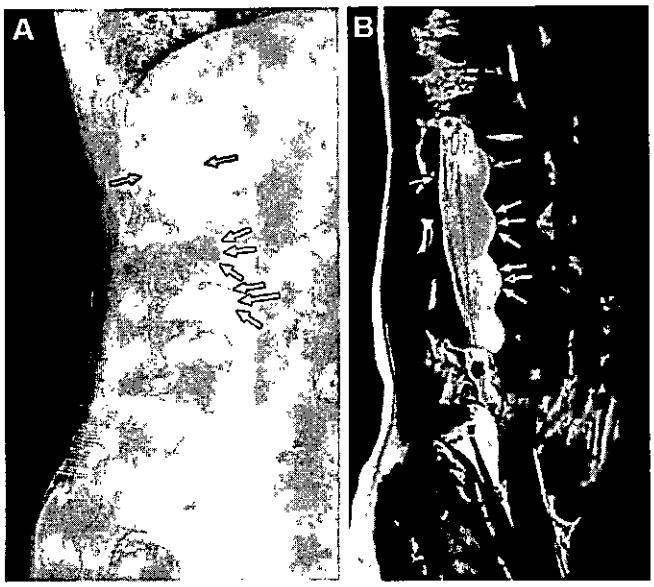

Figure 16. Dural ectasia in a 6-year-old boy with NF1 (same patient as in Fig 9). Lateral radiograph **(A)** and sagittal T2-weighted MR image **(B)** of the lumbar spine show dilatation of the lumbar spinal canal (red arrows) with posterior scalloping of the lumbar vertebral bodies (white arrows).

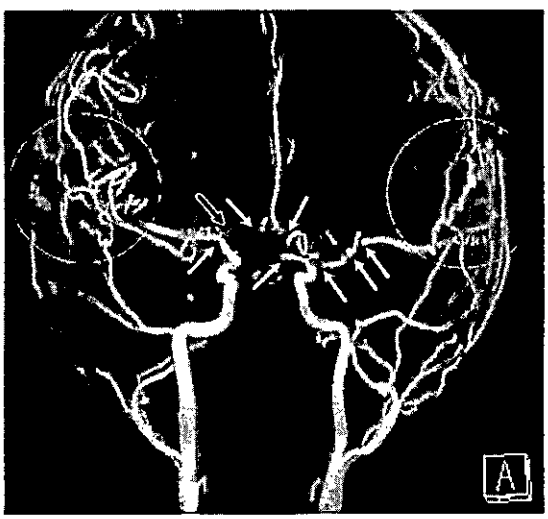

Figure 17. Moyamoya syndrome in an 8-year-old girl with NF1. MR angiogram of the head shows moderate to severe steno-occlusive disease (white arrows) involving the bilateral distal internal carotid arteries and the proximal anterior and middle cerebral arteries. Prominent right-sided basal collaterals (black arrow) resembling a puff of smoke *(moyamoya)* are also noted. The patient had undergone bilateral pial synangiosis, and flow-related signal intensity is seen within the synangiosis vessels (circles).

Figure 18. Noonan syndrome in a fetus at 26 weeks gestation. T2-weighted half-Fourier acquisition single-shot turbo spin-echo (HASTE) MR image of the fetus shows nuchal skin thickening and edema (black arrow), prominent extra-axial spaces (blue arrow), frontal bossing (white arrow), and polyhydramnios.

Figure 19. Hypertrophic obstructive cardiomyopathy in a 13-year-old child with Noonan syndrome. Cardiac MR image shows concentric midventricular hypertrophy of the left ventricle (arrows) with narrowing of the left ventricular outflow tract.

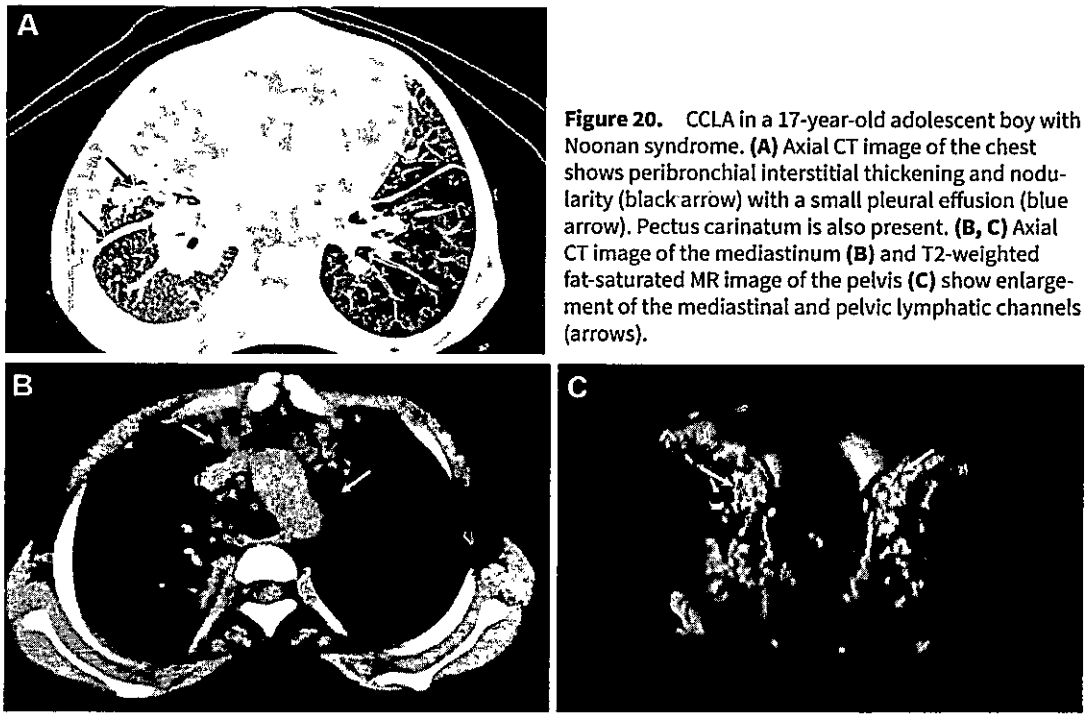

Figure 20. CCLA in a 17-year-old adolescent boy with Noonan syndrome. **(A)** Axial CT image of the chest shows peribronchial interstitial thickening and nodularity (black arrow) with a small pleural effusion (blue arrow). Pectus carinatum is also present. **(B, C)** Axial CT image of the mediastinum **(B)** and T2-weighted fat-saturated MR image of the pelvis **(C)** show enlargement of the mediastinal and pelvic lymphatic channels (arrows).

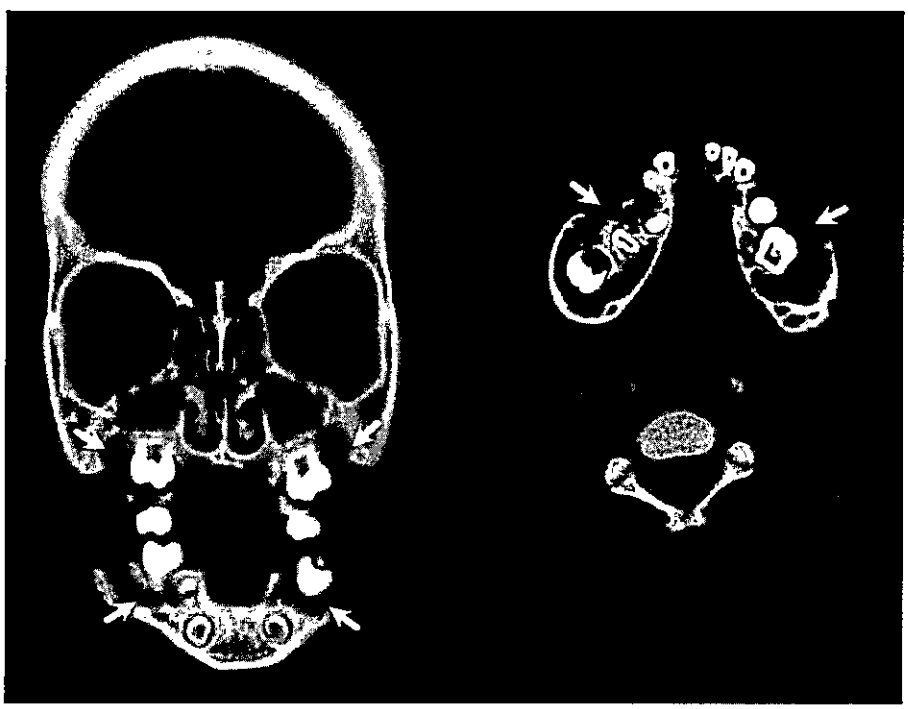

Figure 21. Multiple giant cell lesions (biopsy proven) in the mandible in a 6-year-old boy with Noonan syndrome. Coronal (left) and axial (right) CT images of the face show multiple expansile lucent lesions (arrows) involving the maxilla and mandible.

the molecular common thread, it is now speculated that all giant cell lesions in the jaw and cherubism-like gnathic lesions are related to RASopathies (49).

Overlapping manifestations between NF1 and Noonan syndrome are also seen in other systems as well. For example, moyamoya syndrome is occasionally seen with NF1 and is reported in patients with Noonan syndrome as well (50).

Costello Syndrome

Costello syndrome is an autosomal dominant disorder (51), affecting one in 300 000 live births. It is caused by a de novo gain-of-function mutation in *HRAS* (52,53). Most patients (80%) have the same missense mutation (p.G12S), which causes a constitutive activation of the RAS protein and complex dysregulation of the Ras/MAPK pathway.

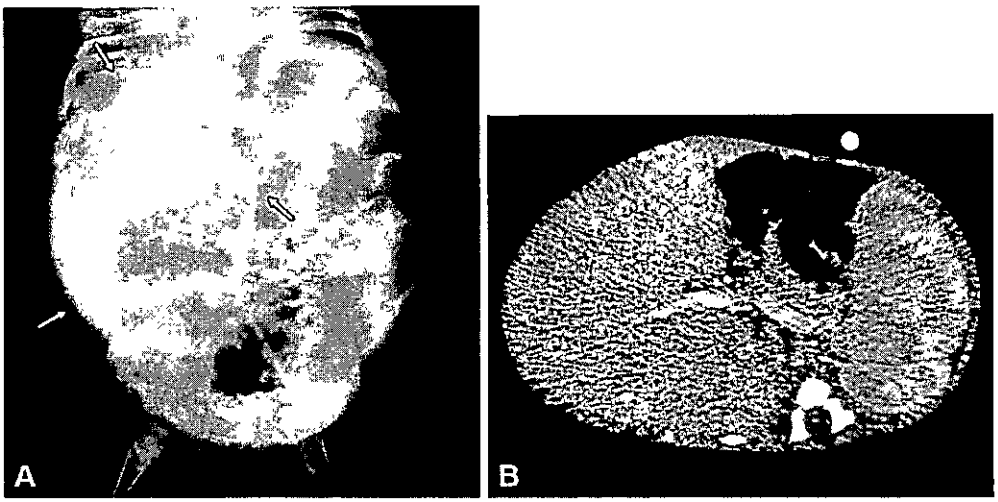

Figure 22. JMML in a 3-month-old boy with Noonan syndrome. **(A)** Frontal abdominal radiograph shows marked enlargement of the liver (arrows). **(B)** Axial CT image of the abdomen with intravenous contrast material shows marked hepatosplenomegaly.

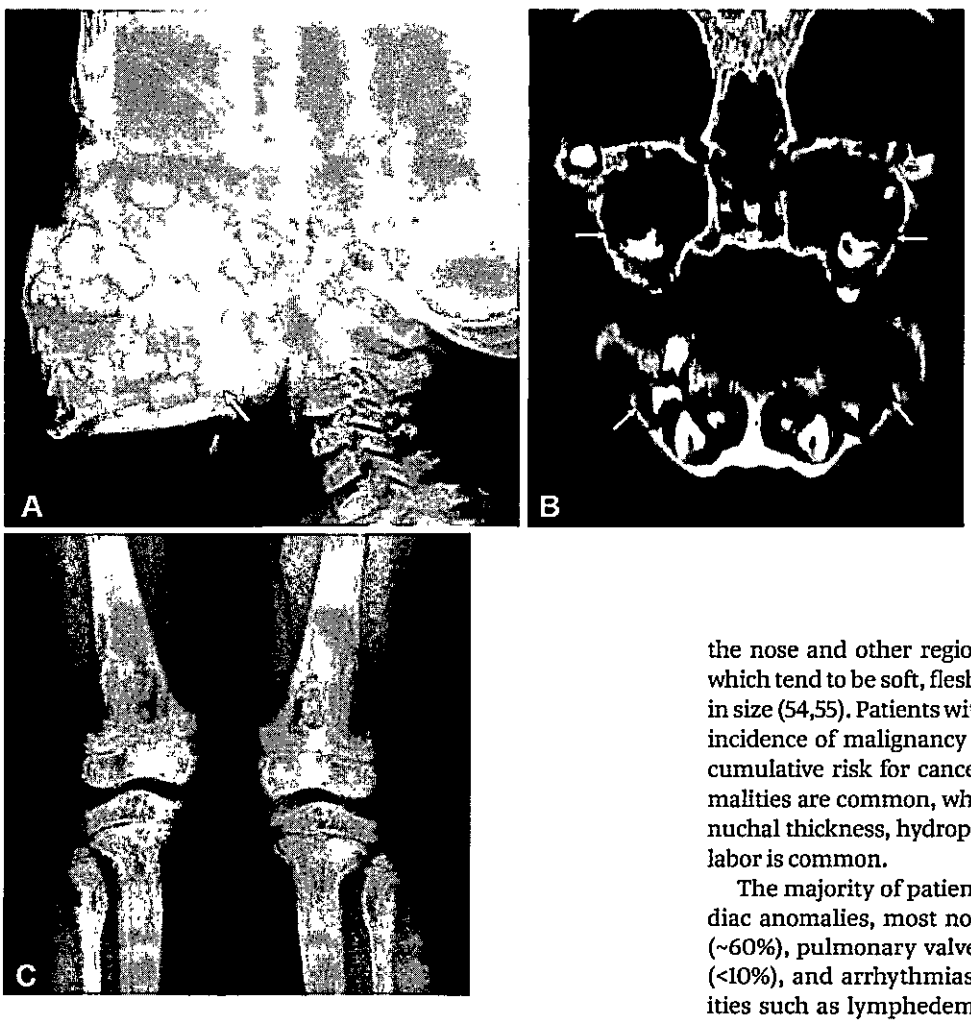

Figure 23. Multiple giant cell lesions in the mandible and maxilla with multiple nonossifying fibromas in a patient with Jaffe-Campanacci syndrome. **(A, B)** Lateral radiograph **(A)** and coronal CT image **(B)** of the face show multiple expansile lucent lesions involving the maxilla and mandible (arrows). **(C)** Frontal radiograph of the knees shows multiple well-defined, cortical-based, lytic lesions with sclerotic margins (arrows) in the distal femora and proximal tibias, consistent with nonossifying fibromas.

The major symptoms of Costello syndrome partially overlap with those of Noonan syndrome: failure to thrive and postnatal growth failure, facial abnormalities, intellectual disability, central nervous system abnormalities, and hypotonia. A distinctive feature is cutaneous papillomas, most commonly in the nose and other regions (face, ear, and perineal regions), which tend to be soft, flesh colored, and approximately 3–4 mm in size (54,55). Patients with Costello syndrome also have a high incidence of malignancy among the RASopathies, with a 15% cumulative risk for cancer by age 20 years (44). Fetal abnormalities are common, which include macrocephaly, increased nuchal thickness, hydrops, and polyhydramnios (56). Preterm labor is common.

The majority of patients with Costello syndrome have cardiac anomalies, most notably hypertrophic cardiomyopathy (~60%), pulmonary valve stenosis (15%–20%), septal defects (<10%), and arrhythmias (>50%) (57). Lymphatic abnormalities such as lymphedema can occasionally be seen (Fig 24) (41). Papillomas can affect the urinary bladder (Fig 25) as well as the skin. Bladder papillomas may evolve into transitional cell carcinoma in late childhood to adulthood.

Musculoskeletal features include hand dysfunction, ulnar deviation of the wrist, elbow or shoulder joint contractures, hip dysplasia, foot deformity, and scoliosis (58,59).

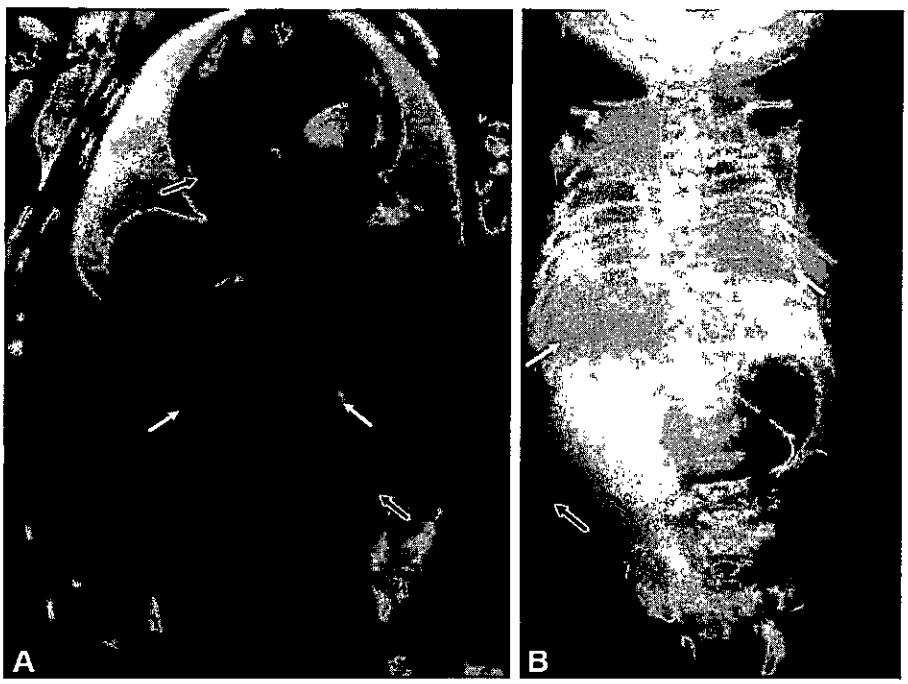

Figure 24. Chylothorax and generalized lymphedema in a fetus with Costello syndrome (diagnosed postnatally). Fetal MR image **(A)** and image from subsequent portable chest-abdomen radiography **(B)** show bilateral pleural effusions (white arrows) and generalized body wall edema (black arrows). (Case courtesy of Shunsuke Nosaka, MD, PhD, Tokyo, Japan.)

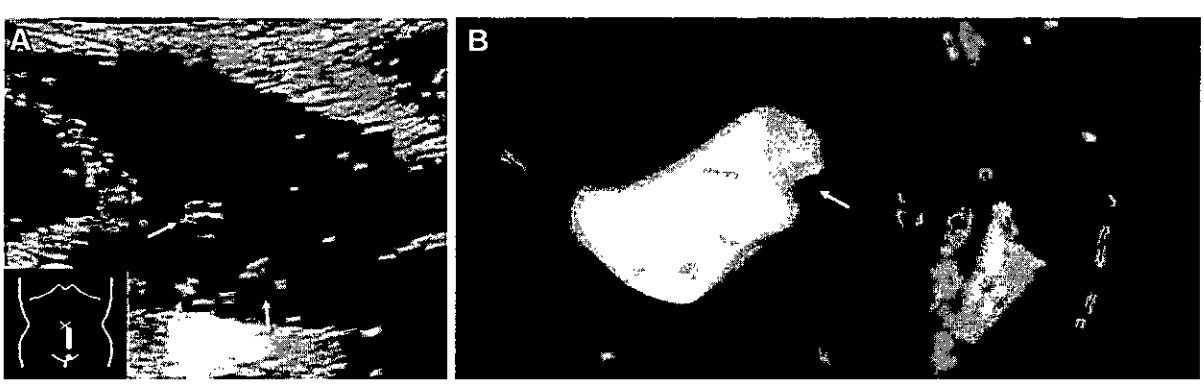

Figure 25. Bladder papillomatosis in a 7-year-old boy with Costello syndrome. **(A)** US image of the bladder shows multiple papillomas (arrows) in the bladder. **(B)** Sagittal T2-weighted fat-saturated MR image of the pelvis shows papillomas (arrow) along the posterior bladder wall.

CFC Syndrome

CFC syndrome is an autosomal dominant disorder with many overlapping features with Noonan syndrome and Costello syndrome (60,61). Although the exact prevalence is unknown, it is estimated to be one in 810 000 newborns in Japan. It is caused by de novo gain-of-function mutations downstream of the Ras/MAPK signaling pathway: *BRAF* (most common, ~75%; higher incidence of pulmonary stenosis and hypertrophic cardiomyopathy), *MEK1*, *MEK2*, and *KRAS* (causes both CFC syndrome and Noonan syndrome) (62,63). These different mutations appear to result in dysregulation of MAPK signaling in common and thus similar phenotypic consequences.

The major symptoms of CFC syndrome include characteristic facies, prominent skin findings (melanocytic nevi, keratosis pilaris, sparse curly hair), failure to thrive and poor growth, hypotonia, seizures, and intellectual disability (64–66). Prenatal abnormalities at US include increased nuchal thickness, cystic hygroma, and polyhydramnios. Premature birth is present in up to half of pregnancies. Because of the clinical overlap with Noonan syndrome and Costello syndrome, diagnosis can be challenging, especially in the newborn period.

Cardiac abnormalities are frequent (~75%), like in Noonan syndrome and Costello syndrome, with the most prevalent being pulmonary valve stenosis (~45%), hypertrophic cardiomyopathy (~40%), and septal defects (atrial septal defect in 18%–28%, ventricular septal defect in 11%–22%) (61). Hypertrophic cardiomyopathy in CFC syndrome can have a wide variation in severity, ranging from the rapidly progressive lethal type to the nonprogressive mild type. Like Noonan syndrome, CFC syndrome can also be associated with lymphatic abnormalities such as lymphedema (41).

Musculoskeletal features include hypertonia, joint contractures, scoliosis, and pes planovalgus (58). Patients with CFC syndrome are not at risk for malignancy (44).

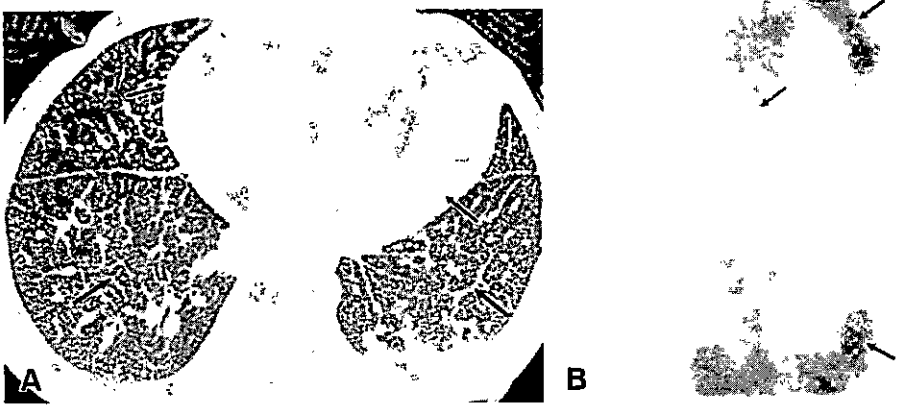

Figure 26. CCLA in a 12-year-old girl with CFC syndrome. **(A)** Axial CT image of the lungs shows bilateral interstitial thickening (black arrows) secondary to lymphangiectasia. There is also pericardial effusion (blue arrows) and cardiomegaly. **(B)** Image from nuclear medicine lymphoscintigraphy shows hypoplasia of the thoracic duct (red arrow) and abnormal lymphatic reflux to the lung, pleural cavity, and retroperitoneum (black arrows).

Central Conducting Lymphatic Anomaly

CCLA is a recently established disease entity and a recent addition to the RASopathies after discovery of the causative genes *ARAF* and *EPHB4* in the Ras/MAPK pathway (67). CCLA is caused by dysfunction of the central lymphatic channels, involving either the thoracic duct or cisterna chyli. Poorly developed atretic central lymphatic channels lead to chronic reflux of lymphatic fluid into the surrounding tissues in the chest and abdomen, leading to pleural effusions, pericardial effusions, ascites, and generalized lymphedema, which can subsequently result in organ dysfunction, protein loss, and infections. MR lymphangiography can be useful in diagnosis, showing enlargement of lymphatic channels (lymphangiectasia), lymphatic fluid reflux, and failure to empty into the thoracic duct or subclavian vein at the thoracic duct outlet (Fig 26).

CM-AVM Syndrome

CM-AVM syndrome is an autosomal dominant disorder characterized by multifocal capillary malformations often in association with fast-flow vascular lesions (arteriovenous malformations and fistulas), most commonly in the central nervous system (68,69). It affects up to one in 100 000 live births. It is caused by heterozygous loss-of-function mutations in *RASA1* (CM-AVM1 syndrome) (70) and *EPHB4* (CM-AVM2 syndrome) (71). Mutations in either of the genes result in constitutive activation of the Ras/MAPK and Ras/Ak strain transforming (AKT)/mammalian target of rapamycin (mTOR) pathways, leading to abnormal differentiation of endothelial cells and disorganized vascular development.

CM-AVM2 syndrome mimics CM-AVM1 syndrome but is also often associated with clinical features resembling those of hereditary hemorrhagic telangiectasia (HHT). HHT manifests with hepatic and pulmonary arteriovenous malformations as well as cutaneous and mucosal telangiectases. Parkes Weber syndrome can be seen with both CM-AVM1 and CM-AVM2 syndromes.

The major clinical symptoms are restricted to the lymphatic and vascular systems. A clinical hallmark is numerous pinkish macules in the skin, which actually represent cutaneous micro–arteriovenous malformations (Fig 27). Fast-flow vascular malformations can occur in many tissues, including the skin, muscle, bone, brain, and spinal cord, which may be complicated by cardiac overload.

Fast-flow intracranial lesions include not only arteriovenous malformations and arteriovenous fistulas but also vein of Galen aneurysmal malformation (72). In fact, it is known that vein of Galen aneurysmal malformation is associated with two vascular malformation syndromes: one is CM-AVM (mutations in *RASA1*) (Fig 28), and the other is HHT (mutations in *ENG* or *ACVRL1*). Yet, individuals with mutations of these genes probably represent only a small fraction of all cases with vein of Galen aneurysmal malformation. Brain and spine MRI can help identify fast-flow intracranial lesions in patients with CM-AVM syndrome (73).

It should be noted that vascular anomalies have been extensively studied and reclassified recently (International Society for the Study of Vascular Anomalies [ISSVA] classification), and CM-AVM syndrome is one of those diseases as well.

Potential Therapies

The Ras/MAPK pathway has been well studied in the context of cancer and its treatment (1,74). Somatic mutations (as opposed to the germline mutations) in the Ras/MAPK pathway have been known to cause many types of cancers and are observed in up to 16% of cancers (75). However, the number of malignancies seen in RASopathy patients with germline mutations is limited, and a full spectrum of malignancies caused by somatic mutations are not seen in RASopathy patients. The reason for this is still poorly understood.

Molecular inhibition of the pathway (eg, mitogen-activated protein kinase kinase [MEK] inhibitors) has been proved to be promising for cancer treatment (Fig 29). Historically, patients with RASopathies only had symptomatic treatment options. However, identification of the causative genes and pathophysiology has opened a gate to strategic new therapies with a focus on intervening in the Ras/MAPK pathway. It may

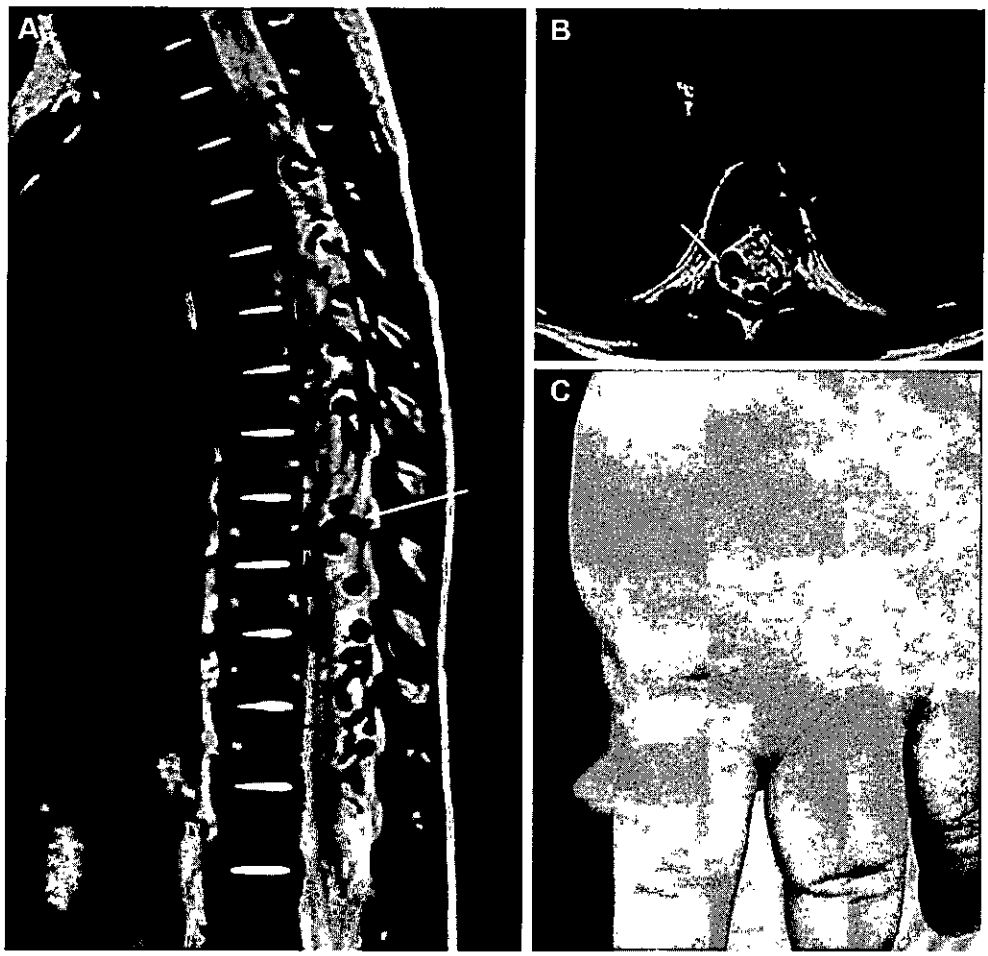

Figure 27. Spinal dural arteriovenous fistulas in a 2-year-old girl with a family history of CM-AVM. **(A,B)** Sagittal **(A)** and axial **(B)** T2-weighted MR images show multiple serpentine intradural extramedullary flow voids affecting a long segment of the thoracolumbar spine (white arrow). There is associated spinal cord edema (blue arrow). **(C)** Photograph shows a pinkish macule in the skin of a sibling of the patient who has the same disorder.

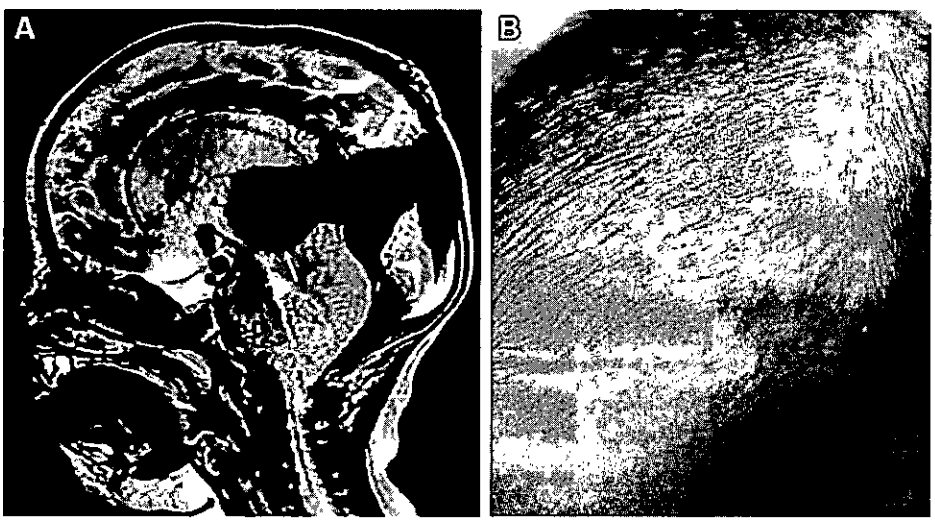

Figure 28. Vein of Galen aneurysmal malformation in a 6-month-old boy with CM-AVM syndrome. **(A)** Sagittal T2-weighted MR image of the brain shows prominent arteries (red arrow) supplying a markedly enlarged median prosencephalic vein (white arrow) and enlarged falcine sinus (blue arrow). **(B)** Photograph shows a pinkish macule in the skin of the patient.

be possible to use modulators for the Ras/MAPK pathway to alleviate some of the complications seen in RASopathies. Early research data show promising results, and these treatments may become a standard of care in the future.

Conclusion

This article reviewed the concept of RASopathies and their imaging spectrum. There are overlapping features among various RASopathies, consistent with the common genetic

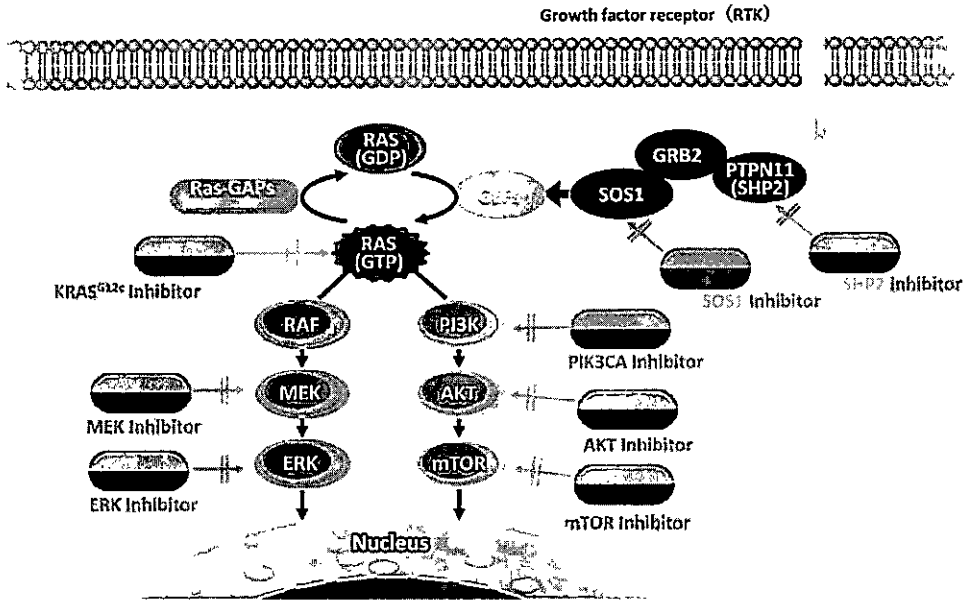

Figure 29. Potential therapies. Molecular inhibition of the Ras/MAPK pathway has proved to be a promising strategy for cancer treatment, and it may be possible to use the same modulators for noncancerous RASopathies to alleviate some complications. *AKT* = Ak strain transforming, *ERK* = extracellular signal-regulated kinase, *GAPs* = GTPase-activating proteins, *GDP* = guanosine diphosphate, *GEFs* = guanine nucleotide exchange factors, *GTP* = guanosine triphosphate, *MEK* = mitogen-activated protein kinase kinase, *mTOR* = mammalian target of rapamycin, *PI3K* = phosphoinositide 3-kinase, *RAF* = rapidly accelerated fibrosarcoma, *RTK* = receptor tyrosine kinase.

pathway contributing to this group of disorders. Unique features among RASopathies may be due to complex interactions and additional supplementary pathways.

Clinicians are starting to treat patients with RASopathies in comprehensive multidisciplinary clinics, and effective therapeutic interventions for RASopathies may become available in the future. Radiologists should also be aware of the concept of RASopathies and the imaging findings of this group of disorders. This recently established entity is still under research, and new findings are being discovered. Knowledge of RASopathies can also help identify subtle lesions and may help clarify yet unknown manifestations.

Author affiliations.—From the Department of Radiology, Boston Children's Hospital, Harvard Medical School, 300 Longwood Ave, Boston, MA 02115 (A.H., S.A.C.); Department of Radiology, Keio University School of Medicine, Tokyo, Japan (Y.T., T.N., M.J.); Department of Radiology, Tokyo Metropolitan Children's Medical Center, Tokyo, Japan (Y.T., T.K.); Department of Radiology, Musashino-Yowakai Hospital, Tokyo, Japan (G.N.); and Department of Radiology, University of Iowa Hospitals and Clinics, Iowa City, Iowa (T.H., T.S.S., Y.S.). Presented as an education exhibit at the 2022 RSNA Annual Meeting. Received May 23, 2023; revision requested July 26 and received August 1; accepted September 7. **Address correspondence to** A.H. (email: *atsuhiko.handa@childrens.harvard.edu*).

Disclosures of conflicts of interest.—**Y.S.** Editorial board member of *RadioGraphics*. All other authors, the editor, and the reviewers have disclosed no relevant relationships.

References

1. Rauen KA. The RASopathies. Annu Rev Genomics Hum Genet 2013;14(1):355–369.
2. Rauen KA. Defining RASopathy. Dis Model Mech 2022;15(2):dmm049344.
3. Fowlkes JL, Thrailkill KM, Bunn RC. RASopathies: the musculoskeletal consequences and their etiology and pathogenesis. Bone 2021;152:116060.
4. Cawthon RM, O'Connell P, Buchberg AM, et al. Identification and characterization of transcripts from the neurofibromatosis 1 region: the sequence and genomic structure of EVI2 and mapping of other transcripts. Genomics 1990;7(4):555–565.
5. Viskochil D, Buchberg AM, Xu G, et al. Deletions and a translocation interrupt a cloned gene at the neurofibromatosis type 1 locus. Cell 1990;62(1):187–192.
6. Wallace MR, Marchuk DA, Andersen LB, et al. Type 1 neurofibromatosis gene: identification of a large transcript disrupted in three NF1 patients. Science 1990;249(4965):181–186.
7. Miller DT, Freedenberg D, Schorry E, et al; American College of Medical Genetics and Genomics. Health Supervision for Children with Neurofibromatosis Type 1. Pediatrics 2019;143(5):e20190660.
8. Tamura R. Current Understanding of Neurofibromatosis Type 1, 2, and Schwannomatosis. Int J Mol Sci 2021;22(11):5850.
9. Williams VC, Lucas J, Babcock MA, Gutmann DH, Korf B, Maria BL. Neurofibromatosis type 1 revisited. Pediatrics 2009;123(1):124–133.
10. Dunnett-Kane V, Burkitt-Wright E, Blackhall FH, Malliri A, Evans DG, Lindsay CR. Germline and sporadic cancers driven by the RAS pathway: parallels and contrasts. Ann Oncol 2020;31(7):873–883.
11. Patel NB, Stacy GS. Musculoskeletal manifestations of neurofibromatosis type 1. AJR Am J Roentgenol 2012;199(1):W99–W106.
12. Friedman JM, Arbiser J, Epstein JA, et al. Cardiovascular disease in neurofibromatosis 1: report of the NF1 Cardiovascular Task Force. Genet Med 2002;4(3):105–111.
13. Forman N, Sinskey J, Shalabi A. A Review of Middle Aortic Syndromes in Pediatric Patients. J Cardiothorac Vasc Anesth 2020;34(4):1042–1050.
14. Schürch W, Messerli FH, Genest J, et al. Arterial hypertension and neurofibromatosis: renal artery stenosis and coarctation of abdominal aorta. Can Med Assoc J 1975;113(9):879–885.
15. Lin AE, Birch PH, Korf BR, et al. Cardiovascular malformations and other cardiovascular abnormalities in neurofibromatosis 1. Am J Med Genet 2000;95(2):108–117.
16. Alves Júnior SF, Zanetti G, Alves de Melo AS, et al. Neurofibromatosis type 1: state-of-the-art review with emphasis on pulmonary involvement. Respir Med 2019;149:9–15.
17. Spinnato P, Facchini G, Tetta C, et al. Neurofibromatosis type 1-associated diffuse lung disease in children. Pediatr Pulmonol 2019;54(11):1760–1764.
18. Patchefsky AS, Atkinson WG, Hoch WS, Gordon G, Lipshitz HI. Interstitial pulmonary fibrosis and von Recklinghausen's disease: an ultrastructural and immunofluorescent study. Chest 1973;64(4):459–464.
19. Elefteriou F, Kolanczyk M, Schindeler A, et al. Skeletal abnormalities in neurofibromatosis type 1: approaches to therapeutic options. Am J Med Genet A 2009;149A(10):2327–2338.
20. Van Royen K, Brems H, Legius E, Lammens J, Laumen A. Prevalence of neurofibromatosis type 1 in congenital pseudarthrosis of the tibia. Eur J Pediatr 2016;175(9):1193–1198. [Published correction appears in Eur J Pediatr 2017;176(7):993.]
21. Crawford AH, Parikh S, Schorry EK, Von Stein D. The immature spine in type-1 neurofibromatosis. J Bone Joint Surg Am 2007;89(suppl 1):123–142.
22. Rossi SE, Erasmus JJ, McAdams HP, Donnelly LF. Thoracic manifestations of neurofibromatosis-1. AJR Am J Roentgenol 1999;173(6):1631–1638.
23. Stewart DR, Brems H, Gomes AG, et al. Jaffe-Campanacci syndrome, revisited: detailed clinical and molecular analyses determine whether

patients have neurofibromatosis type 1, coincidental manifestations, or a distinct disorder. Genet Med 2014;16(6):448–459.
24. Baumhoer D, Kovac M, Sperveslage J, et al. Activating mutations in the MAP-kinase pathway define non-ossifying fibroma of bone. J Pathol 2019;248(1):116–122.
25. Friedman JM, Birch PH. Type 1 neurofibromatosis: a descriptive analysis of the disorder in 1,728 patients. Am J Med Genet 1997;70(2):138–143.
26. Jacquemin C, Bosley TM, Liu D, Svedberg H, Buhaliqa A. Reassessment of sphenoid dysplasia associated with neurofibromatosis type 1. AJNR Am J Neuroradiol 2002;23(4):644–648.
27. Calvez S, Levy R, Calvez R, et al. Focal Areas of High Signal Intensity in Children with Neurofibromatosis Type 1: Expected Evolution on MRI. AJNR Am J Neuroradiol 2020;41(9):1733–1739.
28. Lobbous M, Bernstock JD, Coffee E, et al. An Update on Neurofibromatosis Type 1-associated Gliomas. Cancers (Basel) 2020;12(1):114.
29. Polster SP, Dougherty MC, Zeineddine HA, et al. Dural Ectasia in Neurofibromatosis 1: Case Series, Management, and Review. Neurosurgery 2020;86(5):646–655.
30. Sato TS, Handa A, Priya S, Watal P, Becker RM, Sato Y. Neurocristopathies: Enigmatic Appearances of Neural Crest Cell-derived Abnormalities. RadioGraphics 2019;39(7):2085–2102.
31. Brosius SN, Vossough A, Fisher MJ, et al. Characteristics of Moyamoya Syndrome in Pediatric Patients with Neurofibromatosis Type 1. Pediatr Neurol 2022;134:85–92.
32. Gutmann DH, Ferner RE, Listernick RH, Korf BR, Wolters PL, Johnson KJ. Neurofibromatosis type 1. Nat Rev Dis Primers 2017;3(1):17004.
33. Romano AA, Allanson JE, Dahlgren J, et al. Noonan syndrome: clinical features, diagnosis, and management guidelines. Pediatrics 2010;126(4):746–759.
34. Roberts AE, Allanson JE, Tartaglia M, Gelb BD. Noonan syndrome. Lancet 2013;381(9863):333–342.
35. Tartaglia M, Mehler EL, Goldberg R, et al. Mutations in PTPN11, encoding the protein tyrosine phosphatase SHP-2, cause Noonan syndrome. Nat Genet 2001;29(4):465–468. [Published correction appears in Nat Genet 2002;30(1):123.]
36. Razzaque MA, Nishizawa T, Komoike Y, et al. Germline gain-of-function mutations in RAF1 cause Noonan syndrome. Nat Genet 2007; 39(8):1013–1017.
37. Pandit B, Sarkozy A, Pennacchio LA, et al. Gain-of-function RAF1 mutations cause Noonan and LEOPARD syndromes with hypertrophic cardiomyopathy. Nat Genet 2007;39(8):1007–1012.
38. Croonen EA, Nillesen WM, Stuurman KE, et al. Prenatal diagnostic testing of the Noonan syndrome genes in fetuses with abnormal ultrasound findings. Eur J Hum Genet 2013;21(9):936–942.
39. Linglart L, Gelb BD. Congenital heart defects in Noonan syndrome: diagnosis, management, and treatment. Am J Med Genet C Semin Med Genet 2020;184(1):73–80.
40. Calcagni G, Adorisio R, Martinelli S, et al. Clinical Presentation and Natural History of Hypertrophic Cardiomyopathy in RASopathies. Heart Fail Clin 2018;14(2):225–235.
41. Sleutjes J, Kleimeier L, Leenders E, Klein W, Draaisma J. Lymphatic Abnormalities in Noonan Syndrome Spectrum Disorders: A Systematic Review. Mol Syndromol 2022;13(1):1–11.
42. Biko DM, Reisen B, Otero HJ, et al. Imaging of central lymphatic abnormalities in Noonan syndrome. Pediatr Radiol 2019;49(5):586–592.
43. Kleimeier LER, van Schaik C, Leenders E, Itkin M, Klein WM, Draaisma JMT. Lymphatic Phenotype of Noonan Syndrome: Innovative Diagnosis and Possible Implications for Therapy. J Clin Med 2022;11(11):3128.
44. Kratz CP, Rapisuwon S, Reed H, Hasle H, Rosenberg PS. Cancer in Noonan, Costello, cardiofaciocutaneous and LEOPARD syndromes. Am J Med Genet C Semin Med Genet 2011;157C(2):83–89.
45. Strullu M, Caye A, Lachenaud J, et al. Juvenile myelomonocytic leukaemia and Noonan syndrome. J Med Genet 2014;51(10):689–697.
46. Opitz JM, Weaver DD. The neurofibromatosis-Noonan syndrome. Am J Med Genet 1985;21(3):477–490.
47. Ekvall S, Sjörs K, Jonzon A, Vihinen M, Annerén G, Bondeson ML. Novel association of neurofibromatosis type 1-causing mutations in families with neurofibromatosis-Noonan syndrome. Am J Med Genet A 2014;164A(3):579–587.
48. Tartaglia M, Kalidas K, Shaw A, et al. PTPN11 mutations in Noonan syndrome: molecular spectrum, genotype-phenotype correlation, and phenotypic heterogeneity. Am J Hum Genet 2002;70(6):1555–1563.
49. Schreuder WH, van der Wal JE, de Lange J, van den Berg H. Multiple versus solitary giant cell lesions of the jaw: similar or distinct entities? Bone 2021;149:115935.
50. Gupta M, Choudhri OA, Feroze AH, Do HM, Grant GA, Steinberg GK. Management of moyamoya syndrome in patients with Noonan syndrome. J Clin Neurosci 2016;28:107–111.
51. Gripp KW, Morse LA, Axelrad M, et al. Costello syndrome: clinical phenotype, genotype, and management guidelines. Am J Med Genet A 2019;179(9):1725–1744.
52. Aoki Y, Niihori T, Kawame H, et al. Germline mutations in HRAS proto-oncogene cause Costello syndrome. Nat Genet 2005;37(10):1038–1040.
53. Tidyman WE, Rauen KA. Noonan, Costello and cardio-facio-cutaneous syndromes: dysregulation of the Ras-MAPK pathway. Expert Rev Mol Med 2008;10:e37.
54. Rauen KA. HRAS and the Costello syndrome. Clin Genet 2007;71(2): 101–108.
55. Siegel DH, Mann JA, Krol AL, Rauen KA. Dermatological phenotype in Costello syndrome: consequences of Ras dysregulation in development. Br J Dermatol 2012;166(3):601–607.
56. Lin AE, O'Brien B, Demmer LA, et al. Prenatal features of Costello syndrome: ultrasonographic findings and atrial tachycardia. Prenat Diagn 2009;29(7):682–690.
57. Lin AE, Alexander ME, Colan SD, et al. Clinical, pathological, and molecular analyses of cardiovascular abnormalities in Costello syndrome: a Ras/MAPK pathway syndrome. Am J Med Genet A 2011;155A(3):486–507.
58. Reinker KA, Stevenson DA, Tsung A. Orthopaedic conditions in Ras/MAPK related disorders. J Pediatr Orthop 2011;31(5):599–605.
59. Detweiler S, Thacker MM, Hopkins E, Conway L, Gripp KW. Orthopedic manifestations and implications for individuals with Costello syndrome. Am J Med Genet A 2013;161A(8):1940–1949.
60. Rauen KA, Tidyman WE, Estep AL, et al. Molecular and functional analysis of a novel MEK2 mutation in cardio-facio-cutaneous syndrome: transmission through four generations. Am J Med Genet A 2010;152A(4):807–814.
61. Pierpont ME, Magoulas PL, Adi S, et al. Cardio-facio-cutaneous syndrome: clinical features, diagnosis, and management guidelines. Pediatrics 2014;134(4):e1149–e1162.
62. Niihori T, Aoki Y, Narumi Y, et al. Germline KRAS and BRAF mutations in cardio-facio-cutaneous syndrome. Nat Genet 2006;38(3):294–296.
63. Rodriguez-Viciana P, Tetsu O, Tidyman WE, et al. Germline mutations in genes within the MAPK pathway cause cardio-facio-cutaneous syndrome. Science 2006;311(5765):1287–1290.
64. Yoon G, Rosenberg J, Blaser S, Rauen KA. Neurological complications of cardio-facio-cutaneous syndrome. Dev Med Child Neurol 2007;49(12):894–899.
65. Armour CM, Allanson JE. Further delineation of cardio-facio-cutaneous syndrome: clinical features of 38 individuals with proven mutations. J Med Genet 2008;45(4):249–254.
66. Siegel DH, McKenzie J, Frieden IJ, Rauen KA. Dermatological findings in 61 mutation-positive individuals with cardiofaciocutaneous syndrome. Br J Dermatol 2011;164(3):521–529.
67. Li D, March ME, Gutierrez-Uzquiza A, et al. ARAF recurrent mutation causes central conducting lymphatic anomaly treatable with a MEK inhibitor. Nat Med 2019;25(7):1116–1122.
68. Boon LM, Mulliken JB, Vikkula M. RASA1: variable phenotype with capillary and arteriovenous malformations. Curr Opin Genet Dev 2005;15(3):265–269.
69. Valdivielso-Ramos M, Martin-Santiago A, Azaña JM, et al. Capillary malformation-arteriovenous malformation syndrome: a multicentre study. Clin Exp Dermatol 2021;46(2):300–305.
70. Eerola I, Boon LM, Mulliken JB, et al. Capillary malformation-arteriovenous malformation: a new clinical and genetic disorder caused by RASA1 mutations. Am J Hum Genet 2003;73(6):1240–1249.
71. Amyere M, Revencu N, Helaers R, et al. Germline Loss-of-Function Mutations in EPHB4 Cause a Second Form of Capillary Malformation-Arteriovenous Malformation (CM-AVM2) Deregulating RAS-MAPK Signaling. Circulation 2017;136(11):1037–1048.
72. Duran D, Karschnia P, Gaillard JR, et al. Human genetics and molecular mechanisms of vein of Galen malformation. J Neurosurg Pediatr 2018;21(4):367–374.
73. Wooderchak-Donahue WL, Johnson P, McDonald J, et al. Expanding the clinical and molecular findings in RASA1 capillary malformation-arteriovenous malformation. Eur J Hum Genet 2018;26(10):1521–1536.
74. Bos JL. Ras oncogenes in human cancer: a review. Cancer Res 1989;49(17):4682–4689.
75. Prior IA, Lewis PD, Mattos C. A comprehensive survey of Ras mutations in cancer. Cancer Res 2012;72(10):2457–2467.